

<https://doi.org/10.15407/ufm.20.04.551>

V.V. GIRZHON and O.V. SMOLYAKOV

Zaporizhzhya National University,
66 Zhukovsky Str., UA-69600 Zaporizhzhya, Ukraine

MODELLING OF LATTICES OF TWO-DIMENSIONAL QUASI-CRYSTALS

We propose the method for modelling of quasi-periodic structures based on an algorithm being a geometrical interpretation of the Fibonacci-type numerical sequences. The modelling consists in a recurrent multiplication of basis groups of the sites, which possess the 10-th, 8-th or 12-th order rotational symmetry. The advantage of the proposed method consists in an ability to operate with only two-dimensional space coordinates rather than with hypothetical spaces of dimension more than three. The correspondence between the method of projection of quasi-periodic lattices and the method of recurrent multiplication of basis-site groups is shown. As established, the six-dimensional reciprocal lattice for decagonal quasi-crystals can be obtained from orthogonal six-dimensional lattice for icosahedral quasi-crystals by changing the scale along one of the basis vectors and prohibiting the projection of sites, for which the sum of five indices (corresponding to other basis vectors) is not equal to zero. It is shown the sufficiency of using only three indices for describing diffraction patterns from quasi-crystals with 10-th, 8-th and 12-th order symmetry axes. Original algorithm enables direct obtaining of information about intensity of diffraction reflexes from the quantity of self-overlaps of sites in course of construction of reciprocal lattices of quasi-crystals.

Keywords: quasi-periodic structures, Fibonacci sequence, projection method, basis vectors, rotation symmetry, reciprocal lattice.

1. Introduction

One of actual problems of modern solid-state physics is the description of quasi-crystalline materials structure. For the establishment and description of crystal structures, the experimental and theoretical basis is well developed. In the same time, formal extrapolation of laws and methods of classical crystallography to quasi-crystalline structures leads to significant difficulties. For instance, the usage of three Miller indi-

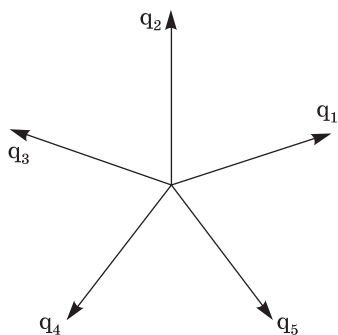


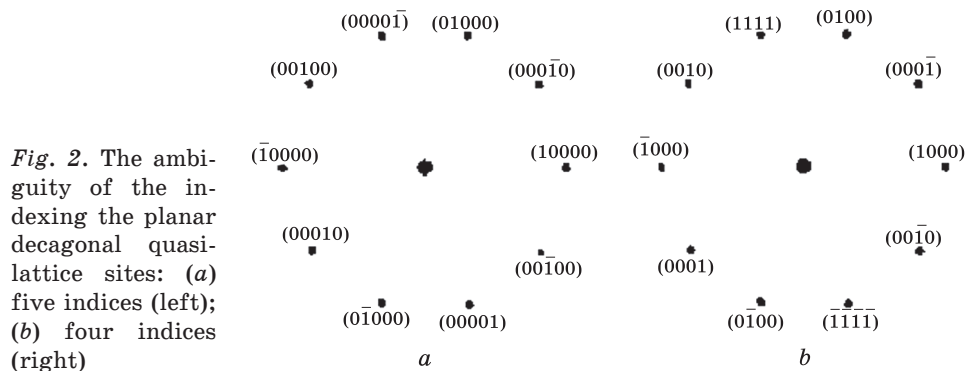
Fig. 1. Basis vectors of planar quasi-lattice with decagonal symmetry

ces for denoting of atomic planes (corresponding to the reciprocal quasi-lattice sites) leads to the fact that these indices are irrational in most cases. In practice, the using of non-integer indices is inconvenient. Therefore, for the indexing of quasi-crystals planes with the symmetry of icosahedron, in paper [1], it was proposed the replacement of three index symbols with six-index integer index as $(h/h' k/k' l/l')$, $H = h + h'\tau$, $K = k + k'\tau$, $L = l + l'\tau$, where irrational constant number $\tau = 2\cos(\pi/5)$ denotes 'golden ratio'.

Another method of indexing of atomic planes is the result of modeling method of icosahedral quasi-crystal structures. It consists in projecting the six-dimensional hypercube lattice on the three-dimensional space [2, 3]. In this method, the six-index designation $(n_1 n_2 n_3 n_4 n_5 n_6)$ was proposed for both atomic planes and reciprocal lattice sites, since the symmetry of quasi-crystal lattice is identic to corresponding symmetry of its reciprocal lattice [4, 5]. In addition, for icosahedral quasi-crystals, authors commonly use the two-index (N, M) -type designation based on the fact that square number of the vector of reciprocal icosahedral quasi-lattice can be presented as [1]

$$Q^2 = N + M\tau. \quad (1)$$

One of the differences of quasi-crystals, which have 8-th, 10-th or 12-th order symmetry axis, from the quasi-crystals with icosahedral symmetry is the periodicity in direction of higher order axis. The corresponding index associated with this direction always accepts integer value and there is no need to replace it with the combination of two indices comprising rational and irrational part. The issue is in ambiguity of assignment of base vectors for flat quasi-lattice, which is perpendicular to symmetry axis of the 8-th, 10-th or 12-th order. In many papers relating to decagonal quasi-crystals [6–10], there are five-index symbols of diffraction reflexes. These symbols include four indices referring to flat quasi-lattice and one index referring to periodicity direction. In papers [11, 12], authors used a six-index notation for such quasi-crystals. In this case, the five-dimensional index refers to flat quasi-lattice. Quite often, *e.g.*, in Refs. [3–15], reflexes are simply denoted as those related to the quasi-crystalline phase without specifying the corresponding indices. The difference in the number of indices is caused by the fact that for the basis vectors of flat reciprocal quasi-lattice are used five vectors, which directed from the pentagon centre to



its vertices $(\pm \mathbf{q}_1, \pm \mathbf{q}_2, \pm \mathbf{q}_3, \pm \mathbf{q}_4, \pm \mathbf{q}_5)$ (Fig. 1). However, considering equation $\mathbf{q}_1 + \mathbf{q}_2 + \mathbf{q}_3 + \mathbf{q}_4 + \mathbf{q}_5 = 0$, obviously, it can be used only four basic vectors. However, the simplification of indexation, which consists in reducing of number of used indices, leads to the fact that equivalent sites of reciprocal quasi-lattice are differently indexed (Fig. 2).

In addition to the problem with indexing, there is also the problem of calculating the diffraction maxima intensity. The main difficulty consists in impossibility of assignment of quasi-crystals elementary cell and, consequently, in impossibility of calculating the structural factor. One way of solving this problem is to approximate quasi-crystalline structure with cubic or other lattices with large parameters [16–19]. However, this method is not convenient, since in order to increase the correspondence of the calculated results to the real one, it is necessary to choose the elementary cells of approximant structure with the largest values of lattice parameters. In this case, the number of cell basis elements naturally increases.

Another method for evaluating the intensity of reflexes is based on the using of periodic lattice in multi-dimensional, in particular, six-dimensional [20] space.

To solve these problems more correctly, the original method of modelling the quasi-periodic structures, elucidated in papers [21–25], is proposed.

2. Decagonal Quasi-Periodic Lattices

Since the concept of the quasi-crystal is closely related to the concepts such as Fibonacci sequence (elements of which are determined by the equation $F_n = F_{n-1} + F_{n-2}$) and the ‘golden ratio’ (expressed by τ number), then, some kind of geometric interpretation of this sequence is suggested for modelling.

For two-dimensional decagonal quasi-lattice, the process of modelling can be demonstrated as follows. The group of sites, set by ten basic vectors $(\pm \mathbf{q}_1, \pm \mathbf{q}_2, \pm \mathbf{q}_3, \pm \mathbf{q}_4, \pm \mathbf{q}_5)$, is selected for the first element of the

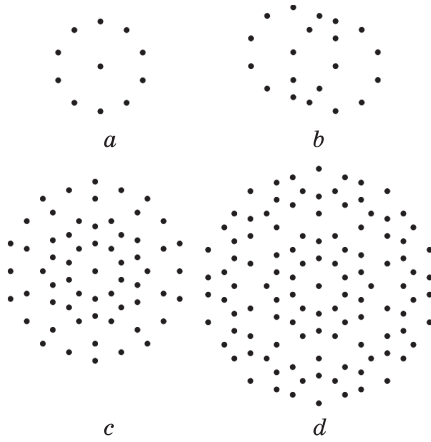


Fig. 3. The process of generation of quasi-lattice sites: (a) initial group of sites, (b) displacement of additional initial group of sites along one of the basis vectors, (c) group of sites D_2 , (d) group of sites D_3

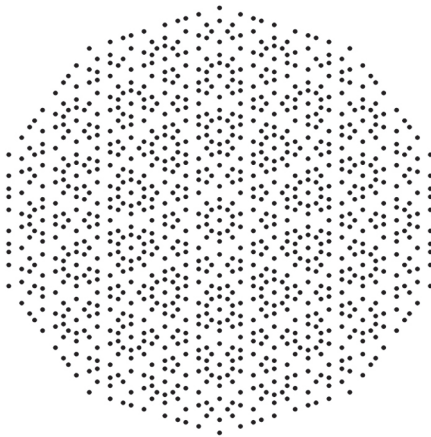


Fig. 4. Group of sites D_4 constructed according to algorithm no. 1

lattice can be written in the form of recursive expression $D_n = D_{n-1} + \{\tau^{n-2}\mathbf{q}_i\}D_{n-2}$. Starting with the third group of sites, it is possible to implement two more versions of recursive algorithm: $D_n = D_{n-2} + \{\tau^{n-2}\mathbf{q}_i\}D_{n-1}$ and $D_n = D_{n-1} + \{\tau^{n-2}\mathbf{q}_i\}D_{n-1}$.

Therefore, we denote the algorithm $D_n = D_{n-1} + \{\tau^{n-2}\mathbf{q}_i\}D_{n-2}$ as algorithm no. 1, $D_n = D_{n-2} + \{\tau^{n-2}\mathbf{q}_i\}D_{n-1}$ as algorithm no. 2, and $D_n = D_{n-1} + \{\tau^{n-2}\mathbf{q}_i\}D_{n-1}$ as algorithm no. 3.

‘sequence’. Let us call this group as D_1 (Fig. 3, a).

To simplify the recording, we denote these ten vectors as \mathbf{q}_i , where i -index varies from 1 to 10. The group D_2 is obtained by placing the centres of additional ten groups D_1 in the sites of the initial group (Fig. 3, b, c). Thus, the group D_2 is the set of sites given by the set of vectors, $\{\mathbf{q}_i\}$, of the previous group, D_1 , and the vectors obtained by the addition of vectors, $\{\mathbf{q}_i + \mathbf{q}_j\}$. Schematically, the procedure for obtaining this group can be written as $D_2 = D_1 + \{\mathbf{q}_i\}D_1$, where the equation $\{\mathbf{q}_i\}D_1$ denotes the shifting the centre of the group D_1 into corresponding vectors. Then, on ends of the vectors $(\pm\tau\mathbf{q}_1, \pm\tau\mathbf{q}_2, \pm\tau\mathbf{q}_3, \pm\tau\mathbf{q}_4, \pm\tau\mathbf{q}_5)$ constructed from the centre of the group D_2 , the centres of the group D_1 are placed. As a result, we obtain the group of sites D_3 (Fig. 3, d) [21, 22].

For obtaining the group D_4 on ends of the vectors $(\pm\tau^2\mathbf{q}_1, \pm\tau^2\mathbf{q}_2, \pm\tau^2\mathbf{q}_3, \pm\tau^2\mathbf{q}_4, \pm\tau^2\mathbf{q}_5)$ constructed from the centre of group D_3 , ten groups D_2 are placed (Fig. 4). Generally, to obtain the group D_n , we have to put the centres of the group D_{n-1} at the ends of the vectors $(\pm\tau^{n-2}\mathbf{q}_1, \pm\tau^{n-2}\mathbf{q}_2, \pm\tau^{n-2}\mathbf{q}_3, \pm\tau^{n-2}\mathbf{q}_4, \pm\tau^{n-2}\mathbf{q}_5)$ constructed from the centre of the group D_{n-2} .

The total algorithm for modelling the decagonal quasi-crystalline

It is known [3, 5, 9] that reciprocal for decagonal quasi-crystalline lattice is also decagonal quasi-periodic lattice. Therefore, obtained models can be compared with electron diffraction patterns of real decagonal quasi-crystals having selected certain scale. In fact, these electron diffraction patterns represent the section of three-dimensional reciprocal lattice.

The quasi-lattice model constructed according to the first algorithm is in a good agreement with the electron diffraction pattern, which was obtained in [26] for the Al–Ni–Co alloy with a decagonal structure (Fig. 5, *a, b*). However, the coincidence of model sites is observed only for reflexes with high and medium intensity. Some of the same low-intensity reflexes according to specified algorithm are not generated. Using the algorithm no. 2 eliminates this problem (Fig. 5, *c*).

Table 1. Characteristics of D_n groups constructed according to three algorithms

Group	Algorithm					
	1		2		3	
	$D_n = D_{n-1} + \{\tau^{n-2}\mathbf{q}_i\}D_{n-2}$		$D_n = D_{n-2} + \{\tau^{n-2}\mathbf{q}_i\}D_{n-1}$		$D_n = D_{n-1} + \{\tau^{n-2}\mathbf{q}_i\}D_{n-1}$	
	Vectors of group	Group radius	Group vectors	Group radius	Group vectors	Group radius
D_1	$\{\mathbf{q}_i\}$	1	$\{\mathbf{q}_i\}$	1	$\{\mathbf{q}_i\}$	1
D_2	$\{\mathbf{q}_i\}, \{\mathbf{q}_i + \mathbf{q}_j\}$	2	$\{\mathbf{q}_i\}, \{\mathbf{q}_i + \mathbf{q}_j\}$	2	$\{\mathbf{q}_i\}, \{\mathbf{q}_i + \mathbf{q}_j\}$	2
D_3	$\{\mathbf{q}_i\}, \{\mathbf{q}_i + \mathbf{q}_j\}, \{\tau\mathbf{q}_i + \mathbf{q}_j\}$	$\tau + 1$	$\{\mathbf{q}_i\}, \{\tau\mathbf{q}_i + \mathbf{q}_j + \mathbf{q}_k\},$	$\tau + 2$	$\{\mathbf{q}_i\}, \{\mathbf{q}_i + \mathbf{q}_j\}, \{\tau\mathbf{q}_i + \mathbf{q}_j\}, \{\tau\mathbf{q}_i + \mathbf{q}_j + \mathbf{q}_k\}$	$\tau + 2$
D_4	$\{\mathbf{q}_i\}, \{\mathbf{q}_i + \mathbf{q}_j\}, \{\tau\mathbf{q}_i + \mathbf{q}_j\}, \{\tau^2\mathbf{q}_i + \mathbf{q}_j\}, \{\tau^2\mathbf{q}_i + \mathbf{q}_j + \mathbf{q}_k\}$	$\tau + 3$	$\{\mathbf{q}_i\}, \{\mathbf{q}_i + \mathbf{q}_j\}, \{\tau^2\mathbf{q}_i + \mathbf{q}_j\}, \{\tau^2\mathbf{q}_i + \tau\mathbf{q}_j + \mathbf{q}_k + \mathbf{q}_l\}$	$2\tau + 3$	$\{\mathbf{q}_i\}, \{\mathbf{q}_i + \mathbf{q}_j\}, \{\tau\mathbf{q}_i + \mathbf{q}_j\}, \{\tau\mathbf{q}_i + \mathbf{q}_j + \mathbf{q}_k\}, \{\tau^2\mathbf{q}_i + \mathbf{q}_l\}, \{\tau^2\mathbf{q}_i + \mathbf{q}_l + \mathbf{q}_k\}, \{\tau^2\mathbf{q}_i + \tau\mathbf{q}_l + \mathbf{q}_j\}, \{\tau^2\mathbf{q}_i + \tau\mathbf{q}_l + \mathbf{q}_j + \mathbf{q}_k\}$	$2\tau + 3$
D_5	$\{\mathbf{q}_i\}, \{\mathbf{q}_i + \mathbf{q}_j\}, \{\tau\mathbf{q}_i + \mathbf{q}_j\}, \{\tau^2\mathbf{q}_i + \mathbf{q}_j\}, \{\tau^2\mathbf{q}_i + \mathbf{q}_j + \mathbf{q}_k\}, \{\tau^3\mathbf{q}_i + \mathbf{q}_j\}, \{\tau^3\mathbf{q}_i + \mathbf{q}_j + \mathbf{q}_k\}, \{\tau^3\mathbf{q}_i + \tau\mathbf{q}_j + \mathbf{q}_k\}, \{\tau^3\mathbf{q}_i + \tau\mathbf{q}_j + \mathbf{q}_k + \mathbf{q}_l\}, \{\tau^3\mathbf{q}_i + \tau\mathbf{q}_j + \mathbf{q}_k\}$	$3\tau + 2$	$\{\mathbf{q}_i\}, \{\tau\mathbf{q}_i + \mathbf{q}_j + \mathbf{q}_k\}, \{\tau^3\mathbf{q}_i + \mathbf{q}_j\}, \{\tau^3\mathbf{q}_i + \mathbf{q}_j + \mathbf{q}_k\}, \{\tau^3\mathbf{q}_i + \tau^2\mathbf{q}_j + \mathbf{q}_k\}, \{\tau^3\mathbf{q}_i + \tau^2\mathbf{q}_j + \tau\mathbf{q}_k + \mathbf{q}_l + \mathbf{q}_m\}$	$4\tau + 4$	$\{\mathbf{q}_i\}, \{\mathbf{q}_i + \mathbf{q}_j\}, \{\tau\mathbf{q}_i + \mathbf{q}_j\}, \{\tau\mathbf{q}_i + \mathbf{q}_j + \mathbf{q}_k\}, \{\tau^2\mathbf{q}_i + \mathbf{q}_l\}, \{\tau^2\mathbf{q}_i + \mathbf{q}_l + \mathbf{q}_k\}, \{\tau^2\mathbf{q}_i + \tau\mathbf{q}_j + \mathbf{q}_k\}, \{\tau^2\mathbf{q}_i + \tau\mathbf{q}_j + \mathbf{q}_k + \mathbf{q}_l\}, \{\tau^3\mathbf{q}_i + \mathbf{q}_j\}, \{\tau^3\mathbf{q}_i + \mathbf{q}_j + \mathbf{q}_k\}, \{\tau^3\mathbf{q}_i + \tau\mathbf{q}_j + \mathbf{q}_k\}, \{\tau^3\mathbf{q}_i + \tau\mathbf{q}_j + \mathbf{q}_k + \mathbf{q}_l\}, \{\tau^3\mathbf{q}_i + \tau^2\mathbf{q}_j + \mathbf{q}_k\}, \{\tau^3\mathbf{q}_i + \tau^2\mathbf{q}_j + \mathbf{q}_k + \mathbf{q}_l\}, \{\tau^3\mathbf{q}_i + \tau^2\mathbf{q}_j + \tau\mathbf{q}_k + \mathbf{q}_l\}, \{\tau^3\mathbf{q}_i + \tau^2\mathbf{q}_j + \tau\mathbf{q}_k + \mathbf{q}_l + \mathbf{q}_m\}$	$4\tau + 4$

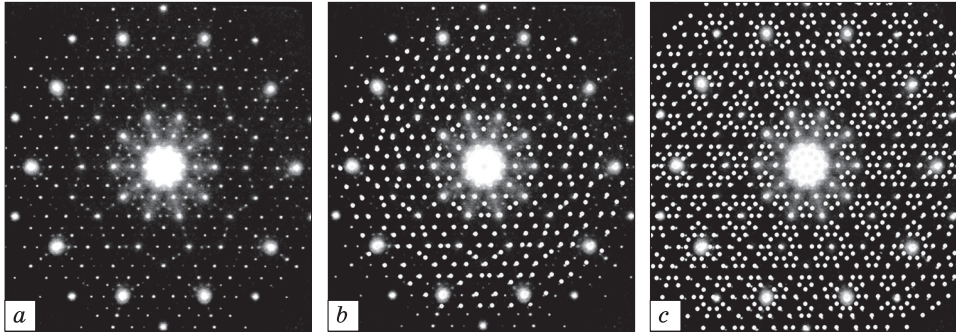


Fig. 5. Overlaying the model groups of lattice sites on electron diffraction pattern of real decagonal Al–Ni–Co quasicrystal [26] (a), where the sites are constructed *via* the algorithms nos. 1 (b) and 2 (c)

Using the algorithm no. 3 also leads to similar result. Some characteristics of sites groups constructed by three specified algorithms are given in Table 1, from which it is evident that the groups constructed according to the algorithm $D_n = D_{n-1} + \tau^{n-2}\mathbf{q}_i D_{n-1}$ (algorithm no. 3) include also those groups, which are constructed according to the two another algorithms.

It should be noted that starting from a group D_3 the last subsets of vectors in algorithms nos. 2 and 3 (Table 1) contain all other ‘preceding’ subsets of corresponding algorithm. For example, the subset of $\{\tau\mathbf{q}_i + \mathbf{q}_j + \mathbf{q}_k\}$ vectors (D_3 group) contains $\{\mathbf{q}_i + \mathbf{q}_j\}$ and $\{\tau\mathbf{q}_i + \mathbf{q}_j\}$ vectors. It can be easily verified, if to consider some properties of basic vectors, particularly that $\mathbf{q}_i + \mathbf{q}_{j+1} = -\tau\mathbf{q}_{i+3}$. At the same time, the last element in groups constructed according to the first proposed algorithm, in the general case, does not contain all subsets. For example, $\{\tau^3\mathbf{q}_i + \mathbf{q}_j + \mathbf{q}_k\}$ subset in D_5 group does not contain $\{\mathbf{q}_i\}$ vectors. It follows from the fact that $|\tau^3\mathbf{q}_i - \tau\mathbf{q}_i - \mathbf{q}_i| > |\mathbf{q}_i|$. Thus, the quasi-lattices constructed according to the second and to the third algorithms are identical with each other and D_n group is reduced to the set of sites given by $\{\mathbf{q}_{i1} + \mathbf{q}_{i2} + \tau\mathbf{q}_{i3} + \tau^2\mathbf{q}_{i4} + \dots + \tau^{n-1}\mathbf{q}_{in}\}$ vectors.

2.1. Relation between Decagonal and Icosahedral Quasi-Lattices; Indexing of Diffraction Reflexes

Writing five unit basis vectors (Fig. 1) in a form

$$\begin{aligned} \mathbf{q}_1 &= \frac{1}{2\tau} \left(\frac{\tau}{\gamma} \mathbf{i} + \mathbf{j} \right), \quad \mathbf{q}_2 = \frac{1}{2\tau} (0\mathbf{i} + 2\tau\mathbf{j}), \quad \mathbf{q}_3 = \frac{1}{2\tau} \left(\frac{\bar{\tau}}{\gamma} \mathbf{i} + \mathbf{j} \right), \\ \mathbf{q}_4 &= \frac{1}{2\tau} \left(\frac{\bar{1}}{\gamma} \mathbf{i} + \bar{\tau}^2 \mathbf{j} \right), \quad \mathbf{q}_5 = \frac{1}{2\tau} \left(\frac{1}{\gamma} \mathbf{i} + \bar{\tau}^2 \mathbf{j} \right), \end{aligned} \quad (2)$$

where $\gamma = 1/\sqrt{\tau + 2}$, then, we can show that, in a case of plain decagonal quasi-lattice, the equation for square distance between the random site and origin of coordinates ($\mathbf{Q} = n_1\mathbf{q}_1 + n_2\mathbf{q}_2 + n_3\mathbf{q}_3 + n_4\mathbf{q}_4 + n_5\mathbf{q}_5$) can be reduced to the form:

$$|\mathbf{Q}|^2 = (n_1^2 + n_2^2 + n_3^2 + n_4^2 + n_5^2 - n_1n_2 - n_2n_3 - n_3n_4 - n_4n_5 - n_5n_1) + (n_1n_2 + n_2n_3 + n_3n_4 + n_4n_5 + n_5n_1 - n_1n_3 - n_2n_4 - n_3n_5 - n_4n_1 - n_5n_2)\tau. \quad (3)$$

Using denotations

$$N^* = n_1^2 + n_2^2 + n_3^2 + n_4^2 + n_5^2 - n_1n_2 - n_2n_3 - n_3n_4 - n_4n_5 - n_5n_1, \\ M^* = n_1n_2 + n_2n_3 + n_3n_4 + n_4n_5 + n_5n_1 - n_1n_3 - n_2n_4 - n_3n_5 - n_4n_1 - n_5n_2, \quad (4)$$

it can be derived the equation, which is similar by the form to obtained in Ref. [1] for icosahedral quasi-crystals:

$$|\mathbf{Q}|^2 = N^* + M^*\tau. \quad (5)$$

Identical form of Eqs. (1) and (5) is due to the relation between icosahedral and decagonal lattices. To prove this statement, let us use the method of projection and select six orthogonal vectors in the reciprocal six-dimensional space, which the general view was reported in Ref. [1]:

$$\begin{aligned} \mathbf{u}_1 &= [\tau \ 1 \ 0 \ 1 \ \bar{\tau} \ 0], \\ \mathbf{u}_2 &= [0 \ \tau \ 1 \ 0 \ 1 \ \bar{\tau}], \\ \mathbf{u}_3 &= [\bar{1} \ 0 \ \tau \ \tau \ 0 \ 1], \\ \mathbf{u}_4 &= [0 \ \bar{\tau} \ 1 \ 0 \ \bar{1} \ \bar{\tau}], \\ \mathbf{u}_5 &= [\tau \ \bar{1} \ 0 \ 1 \ \tau \ 0], \\ \mathbf{u}_6 &= [1 \ 0 \ \tau \ \bar{\tau} \ 0 \ 1], \end{aligned} \quad (6)$$

Let us consider the first triple and the second one of components for each vector as the Cartesian coordinates of reciprocal spaces: physical (XYZ) and 'perpendicular' (X'Y'Z') ones. The vectors (6) determine six vertices of icosahedron both in physical and 'perpendicular' spaces. Thus, the projection of six-dimensional periodic structure constructed on the set of vectors (6) specifies the reciprocal icosahedral lattice. Using rotation matrix of the form

$$\begin{pmatrix} \gamma\tau & 0 & \bar{\gamma} & 0 & 0 & 0 \\ 0 & 1 & 0 & 0 & 0 & 0 \\ \gamma & 0 & \gamma\tau & 0 & 0 & 0 \\ 0 & 0 & 0 & \gamma & 0 & \gamma\tau \\ 0 & 0 & 0 & 0 & 1 & 0 \\ 0 & 0 & 0 & \bar{\gamma}\tau & 0 & \gamma \end{pmatrix}, \quad (7)$$

the system (10) can be converted in a manner that vector \mathbf{u}_6 is projected only onto Z and Z' axis, while projections of the rest of five vectors on XOY and $X'OY'$ planes specifies the vertices of regular pentagon:

$$\begin{aligned}\mathbf{u}_1 &= [\gamma\tau^2 \ 1 \ \gamma\tau \ \gamma \ \bar{\tau} \ \bar{\gamma}\tau], \\ \mathbf{u}_2 &= [\bar{\gamma} \ \tau \ \gamma\tau \ \bar{\gamma}\tau^2 \ 1 \ \bar{\gamma}\tau], \\ \mathbf{u}_3 &= [2\bar{\gamma}\tau \ 0 \ \gamma\tau \ 2\gamma\tau \ 0 \ \bar{\gamma}\tau], \\ \mathbf{u}_4 &= [\bar{\gamma} \ \bar{\tau} \ \gamma\tau \ \bar{\gamma}\tau^2 \ \bar{1} \ \bar{\gamma}\tau], \\ \mathbf{u}_5 &= [\gamma\tau^2 \ \bar{1} \ \gamma\tau \ \gamma \ \tau \ \bar{\gamma}\tau], \\ \mathbf{u}_6 &= [0 \ 0 \ 1/\gamma \ 0 \ 0 \ 1/\gamma].\end{aligned}\quad (8)$$

The set of vectors (8) remains orthogonal, and next statement is correct for both the (8) and (6) vectors:

$$|\mathbf{u}_1| = |\mathbf{u}_2| = |\mathbf{u}_3| = |\mathbf{u}_4| = |\mathbf{u}_5| = |\mathbf{u}_6| = \sqrt{2(\tau + 2)}. \quad (9)$$

Linear combination of the first five vectors (8)

$$\begin{aligned}\mathbf{q}_1^* &= (\mathbf{u}_1 - \mathbf{u}_3), \quad \mathbf{q}_2^* = (\mathbf{u}_2 - \mathbf{u}_4), \quad \mathbf{q}_3^* = (\mathbf{u}_3 - \mathbf{u}_5), \\ \mathbf{q}_4^* &= (\mathbf{u}_4 - \mathbf{u}_1), \quad \mathbf{q}_5^* = (\mathbf{u}_5 - \mathbf{u}_2)\end{aligned}\quad (10)$$

represents five vectors in reciprocal six-dimensional space, which projections onto physical and ‘perpendicular’ spaces are coplanar between each other:

$$\begin{aligned}\mathbf{q}_1^* &= [\tau/\gamma \ 1 \ 0 \ \bar{1}/\gamma\tau \ \bar{\tau} \ 0], \\ \mathbf{q}_2^* &= [0 \ 2\tau \ 0 \ 0 \ 2 \ 0], \\ \mathbf{q}_3^* &= [\bar{\tau}/\gamma \ 1 \ 0 \ 1/\gamma\tau \ \bar{\tau} \ 0], \\ \mathbf{q}_4^* &= [\bar{1}/\gamma \ \bar{\tau}^2 \ 0 \ \bar{1}/\gamma \ 1/\tau \ 0], \\ \mathbf{q}_5^* &= [1/\gamma \ \bar{\tau}^2 \ 0 \ 1/\gamma \ 1/\tau \ 0].\end{aligned}\quad (11)$$

Comparing Eqs. (2) and (11), we can write

$$\mathbf{q}_1 = \frac{1}{2\tau} \mathbf{q}_1^{*\parallel}, \quad \mathbf{q}_2 = \frac{1}{2\tau} \mathbf{q}_2^{*\parallel}, \quad \mathbf{q}_3 = \frac{1}{2\tau} \mathbf{q}_3^{*\parallel}, \quad \mathbf{q}_4 = \frac{1}{2\tau} \mathbf{q}_4^{*\parallel}, \quad \mathbf{q}_5 = \frac{1}{2\tau} \mathbf{q}_5^{*\parallel}; \quad (12)$$

here, $\mathbf{q}_i^{*\parallel}$ are projections of \mathbf{q}_i^* vectors onto reciprocal space.

Thus, the basis vectors $\{\mathbf{q}_i\}$ of reciprocal decagonal quasi-lattice in physical space are expressed through the similar basis vectors of reciprocal icosahedral lattice. Using equations (12), it is possible to obtain the relations between (N^*, M^*) and (N, M) , which appear in Eqs. (1) and (5):

$$N^* + M^*\tau = 1/(2\tau)^2(N + M\tau), \quad N = 4/(N^* + M^*), \quad M = 4/(N^* + 2M^*). \quad (13)$$

Let complement the system (11) with sixth vector and divide all vectors by 2τ :

$$\begin{aligned} \mathbf{q}_1^6 &= [1/2\gamma \quad 1/2\tau \quad 0 \quad \bar{1}/2\gamma\tau^2 \quad \bar{1}/2 \quad 0], \\ \mathbf{q}_2^6 &= [0 \quad 1 \quad 0 \quad 0 \quad 1/\tau \quad 0], \\ \mathbf{q}_3^6 &= [\bar{1}/2\gamma \quad 1/2\tau \quad 0 \quad 1/2\gamma\tau^2 \quad \bar{1}/2 \quad 0], \\ \mathbf{q}_4^6 &= [\bar{1}/2\gamma\tau \quad \bar{\tau}/2 \quad 0 \quad \bar{1}/2\gamma\tau \quad 1/2\tau^2 \quad 0], \\ \mathbf{q}_5^6 &= [1/2\gamma\tau \quad \bar{\tau}/2 \quad 0 \quad 1/2\gamma\tau \quad 1/2\tau^2 \quad 0], \\ \mathbf{q}_6^6 &= [0 \quad 0 \quad \lambda/\sqrt{2}\gamma\tau \quad 0 \quad 0 \quad \lambda/\sqrt{2}\gamma\tau]. \end{aligned} \quad (14)$$

Establishment of dimensionless coefficient λ for vector \mathbf{u}_6 is equivalent to the substitution of the six-dimensional cubic lattice by the orthogonal non-cubic one. It is necessary to note that

$$|\mathbf{q}_1^6| = |\mathbf{q}_2^6| = |\mathbf{q}_3^6| = |\mathbf{q}_4^6| = |\mathbf{q}_5^6| = \sqrt{3-\tau}, \quad |\mathbf{q}_6^6| = \lambda\sqrt{3-\tau}. \quad (15)$$

According to (10) and (14), the indices of random site of reciprocal decagonal lattice ($n_1 \ n_2 \ n_3 \ n_4 \ n_5 \ n_6$) can be expressed through the indices of reciprocal icosahedral (non-cubic) lattice ($k_1 \ k_2 \ k_3 \ k_4 \ k_5 \ k_6$) by next equation:

$$\begin{pmatrix} 1 & 0 & 0 & \bar{1} & 0 & 0 \\ 0 & 1 & 0 & 0 & \bar{1} & 0 \\ \bar{1} & 0 & 1 & 0 & 0 & 0 \\ 0 & \bar{1} & 0 & 1 & 0 & 0 \\ 0 & 0 & \bar{1} & 0 & 1 & 0 \\ 0 & 0 & 0 & 0 & 0 & 1 \end{pmatrix} \begin{pmatrix} n_1 \\ n_2 \\ n_3 \\ n_4 \\ n_5 \\ n_6 \end{pmatrix} = \begin{pmatrix} k_1 \\ k_2 \\ k_3 \\ k_4 \\ k_5 \\ k_6 \end{pmatrix}. \quad (16)$$

It can be easily shown that the sum of the first five indices k_i derived from Eq. (16) is equal to zero.

Thus, the reciprocal decagonal lattice can be constructed by the projection of six-dimensional orthogonal non-cubic lattice (which corresponds to distorted icosahedral lattice) onto the physical space. Additionally, it is necessary to prohibit the projection of sites, in which the sum of the first five indices is not equal to zero.

Considering (14), Eqs. (3) and (5) can be written as

$$\begin{aligned} |\mathbf{Q}|^2 &= (n_1^2 + n_2^2 + n_3^2 + n_4^2 + n_5^2 - n_1n_2 - n_2n_3 - n_3n_4 - n_4n_5 - n_5n_1) + \\ &+ (n_1n_2 + n_2n_3 + n_3n_4 + n_4n_5 + n_5n_1 - n_1n_3 - n_2n_4 - \\ &- n_3n_5 - n_4n_1 - n_5n_2)\tau + \lambda^2n, \end{aligned} \quad (17)$$

$$|\mathbf{Q}^2| = N^* + M^*\tau + \lambda^2L^2, \quad (18)$$

where $N = n_6$.

Table 2. Site indices of the flat decagonal quasi-lattice based on five base vectors and corresponding indices N^* and M^* . The relation between the value of the parameter $\tau N^* - M^*$ and the self-overlapping quantity in the model group D_6

No.	$(n_1 \ n_2 \ n_3 \ n_4 \ n_5)$	N^*	M^*	$ Q $	$\tau N^* - M^*$	Quantity of self-overlaps of sites
1	$(1 \ \bar{1} \ 1 \ 0 \ 0)$	5	-3	$2 - \tau$	11.09	131
2	$(1 \ 0 \ 1 \ 0 \ 0)$	2	-1	$\tau - 1$	4.24	538
3	$(1 \ \bar{1} \ 0 \ 1 \ \bar{1})$	7	-4	$\sqrt{7 - 4\tau}$	15.33	24
4	$(1 \ 0 \ 0 \ 0 \ 0)$	1	0	1	1.62	850
5	$(1 \ \bar{1} \ 0 \ 0 \ 0)$	3	-1	$\sqrt{3 - \tau}$	5.85	424
6	$(2 \ 0 \ 2 \ 0 \ 0)$	8	-4	$2\tau - 2$	16.94	5
7	$(2 \ 0 \ 1 \ 0 \ 0)$	5	-2	$\sqrt{5 - 2\tau}$	10.09	167
8	$(2 \ 0 \ 1 \ 0 \ 1)$	4	-1	$\sqrt{4 - \tau}$	7.47	287
9	$(1 \ 1 \ 0 \ 0 \ 0)$	1	1	τ	0.62	1033
10	$(2 \ \bar{1} \ 1 \ 0 \ 1)$	8	-3	$\sqrt{8 - 3\tau}$	15.94	14
11	$(1 \ 0 \ \bar{1} \ 0 \ 0)$	2	1	$\sqrt{2 + \tau}$	2.24	764
12	$(2 \ \bar{1} \ 0 \ 0 \ 0)$	7	-2	$\sqrt{7 - 2\tau}$	13.33	57
13	$(2 \ 0 \ 0 \ 0 \ 0)$	4	0	2	6.47	347
14	$(1 \ 1 \ \bar{1} \ 0 \ 0)$	3	1	$\sqrt{3 + \tau}$	3.85	514
15	$(1 \ 1 \ \bar{1} \ 0 \ \bar{1})$	5	0	$\sqrt{5}$	8.09	259
16	$(2 \ 0 \ \bar{1} \ 1 \ 0)$	7	-1	$\sqrt{7 - \tau}$	12.33	76
17	$(2 \ 1 \ 0 \ 0 \ 0)$	3	2	$\sqrt{3 + 2\tau}$	2.85	615
18	$(2 \ 0 \ \bar{1} \ 0 \ \bar{1})$	8	-1	$\sqrt{8 - \tau}$	13.94	41
19	$(1 \ 1 \ 0 \ \bar{1} \ 0)$	2	3	$\tau + 1$	0.24	1018
20	$(2 \ 0 \ 1 \ \bar{1} \ \bar{1})$	9	-1	$\sqrt{9 - \tau}$	15.56	15
21	$(2 \ 1 \ 0 \ 0 \ \bar{1})$	6	1	$\sqrt{6 + \tau}$	8.71	216
22	$(2 \ 0 \ 0 \ \bar{1} \ 0)$	5	2	$\sqrt{5 + 2\tau}$	6.09	338
23	$(2 \ \bar{1} \ \bar{1} \ 0 \ 0)$	7	1	$\sqrt{7 + \tau}$	10.33	150
24	$(3 \ 0 \ 0 \ 0 \ 0)$	9	0	3	14.56	27
25	$(1 \ 1 \ 0 \ \bar{1} \ \bar{1})$	3	4	$\sqrt{3 + 4\tau}$	0.85	944
26	$(2 \ \bar{1} \ 0 \ \bar{1} \ 1)$	8	1	$\sqrt{8 + \tau}$	11.94	80
27	$(2 \ 1 \ \bar{1} \ 0 \ 0)$	5	3	$\sqrt{5 + 3\tau}$	5.09	405
28	$(2 \ 2 \ 0 \ 0 \ 0)$	4	4	2τ	2.47	623

Proceeding from the above, it can be proposed quadratic form for decagonal lattice:

$$\frac{1}{d^2} = \frac{N^* + M^* \tau + \lambda^2 L^2}{a^2} = \frac{N^* + M^* \tau}{a^2} + \frac{L^2}{c^2}, \quad \frac{c}{a} = \frac{1}{\lambda}. \quad (19)$$

Using equations (4) and (18), it is possible to proceed from the six-indexes' notation ($n_1 \ n_2 \ n_3 \ n_4 \ n_5 \ n_6$) to the three-indexes' one (NML), which is more convenient in the case of indexing the XRD-patterns of polycrystalline samples. The values of N and M for the plain quasi-lattice are presented in Table 2 in ascending order of $|Q|$. Equation (19) is formally identical to quadratic form for tetragonal lattice.

2.2. Intensity of Diffraction Reflexes

In paper [1], it has been shown that, for icosahedral quasi-crystals, the intensity of diffraction reflexes is determined by the value of $\tau(\tau N - M)$ that is the distance between the site of hyper-lattice and its corresponding projection onto physical space. Moreover, the intensity increases with decreasing of this distance. In our case of two-dimensional decagonal quasi-lattice, the distance from the site of six-dimensional lattice to physical space is determined by modulus of vector:

$$\mathbf{Q}_\perp = n_1 \mathbf{q}_1^\perp + n_2 \mathbf{q}_2^\perp + n_3 \mathbf{q}_3^\perp + n_4 \mathbf{q}_4^\perp + n_5 \mathbf{q}_5^\perp, \quad (20)$$

where \mathbf{q}_i^\perp are projections of six-dimensional vectors (14) onto 'perpendicular' space. Using the set of Eqs. (14), it can be shown that the square value of \mathbf{Q}_\perp modulus can be expressed through the same parameters N^* and M^* , which determine the square value of vector modulus in physical space (5):

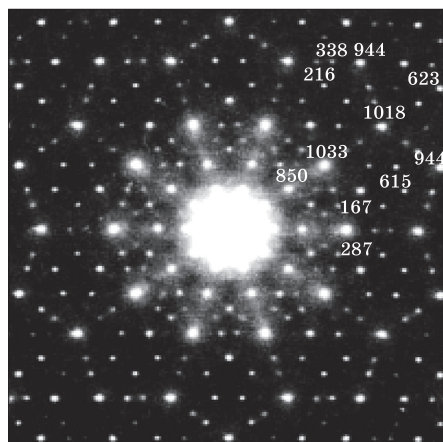
$$|\mathbf{Q}_\perp|^2 = \tau^3(N^* \tau + M^*). \quad (21)$$

Therewith, the square value of six-dimensional vector modulus is equal to 1.5

$$|\mathbf{Q}|^2 = |\mathbf{Q}|^2 + |\mathbf{Q}_\perp|^2 (3 - \tau)(N^* + M^*). \quad (22)$$

It occurs multiple overlapping of sites during modelling the two-dimensional decagonal lattice according to definite algorithm since various combinations of basis vectors can lead to the same result.

Fig. 6. Correlation between the intensity of reflexes on electron diffraction pattern from decagonal Al-Ni-Co quasicrystal [26] and the quantity of self-overlaps of sites at the construction of the quasi-lattice according to algorithm no. 3 (group of sites D_6)



Computer analysis of constructed lattices allowed indicating distinct correlation between the value of $(N^*_{\tau} - M^*)$ parameter, experimental intensity of reflexes and the number of overlaps (Fig. 6, Table 2). The revealed correlation evidences for correctness of the selection of six-dimensional lattice basis vectors (14) that is in agreement with the data of paper [1] for icosahedral lattice. The selection of alternative basis, which projection onto the physical space also determines the vectors (6), may interrupt this correlation. For example, in paper [27], it has been proposed orthogonal basis in five-dimensional space:

$$\begin{aligned} \mathbf{q}_1^5 &= [c_0 \ s_0 \ c_0 \ s_0 \ 1/\sqrt{2}], \\ \mathbf{q}_2^5 &= [c_1 \ s_1 \ c_3 \ s_3 \ 1/\sqrt{2}], \\ \mathbf{q}_3^5 &= [c_2 \ s_2 \ c_1 \ s_1 \ 1/\sqrt{2}], \\ \mathbf{q}_4^5 &= [c_3 \ s_3 \ c_4 \ s_4 \ 1/\sqrt{2}], \\ \mathbf{q}_5^5 &= [c_4 \ s_4 \ c_2 \ s_2 \ 1/\sqrt{2}], \end{aligned} \quad (23)$$

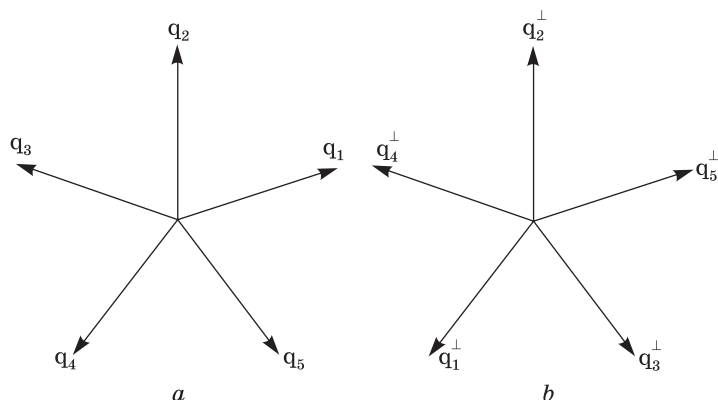
where $c_r = \cos(2r\pi/5)$, $s_r = \sin(2r\pi/5)$, and the first two vectors components are referred to the physical space, while the rest ones are referred to ‘perpendicular’ space. In this case, correlation between the distance from the site of five-dimensional lattice to physical space and the intensity has not been observed.

Comparing systems (14) and (23), we can propose the criterion for selection of decagonal-lattice basis vectors in the space with dimensionality, which is higher than 3: the sum of five basis vectors has to be equal to zero.

Correlation between the intensity of reflexes and the number of overlapping could be interpreted in the following way. Basis sites of quasi-crystalline lattice are obtained from the projection of hyper-lattice sites ‘closely’ located to physical space. Moreover, according to Eq. (26) and Table 2, (10100)- and (10000)-type sites are located at the same minimal distance from coordinate start in six-dimensional space. However, the (10000)-type sites are ‘closer’ located to physical space and this determines their selection as the basis ones. The only one site of six-dimensional hyper-lattice, which located in the real (physical) space, is the origin of coordinate. This is necessary condition of aperiodicity of this hyper-lattice projection in any direction.

In fact, the overlapping of geometric group shifted by certain vector means ‘parallel transfer’ of physical space so that another site of hyper-lattice closely located to the physical space is turned out in the real space (this site corresponds to $\tau^{n-2}\mathbf{q}_i$ vector). Intensity of diffraction reflexes is determined by the distance from the hyper-lattice site to physical space [20]. Since that, indicated correlation of intensity can be

Fig. 7. Mutual orientation of basis vectors in the physical (a) and 'perpendicular' (b) spaces



interpreted in terms of probability for hyper-lattice site to be in projection region at the 'shifting' of the physical space during the generation of sites groups. In this manner, within this algorithm, the sites located closer to the initial physical space are generated more frequently as compared to those located at higher distances. Therefore, multiple generation of the same sites enables to get information on the intensity of appropriate diffraction reflexes.

Figure 7 illustrates mutual orientation of the basis vectors projections onto the physical \mathbf{q}_i and 'perpendicular' \mathbf{q}_i^\perp spaces according to the set (14).

Value of $\mathbf{q}_1 + \mathbf{q}_2 = -\tau \mathbf{q}_4$ type defines one of the shifting the group of sites during modelling process. It corresponds to 'perpendicular' shifting to $\mathbf{q}_1^\perp + \mathbf{q}_2^\perp = -\mathbf{q}_4^\perp/\tau$ vector. It follows that the radii of sites groups in the model (algorithms nos. 2 and 3) in the physical and 'perpendicular' spaces are defined by equations:

$$r_n = 1 + 1 + \tau + \dots + \tau^{n-2}, \quad r_n^\perp = 1 + 1 + 1/\tau + \dots + 1/\tau^{n-2}, \quad (24)$$

respectfully. The second equation in (24) shows that the radius of sites groups in 'perpendicular' space is limited:

$$r_{n \rightarrow \infty}^\perp = 1 + (1 - 1/\tau)^{-1} = 1 + \tau^2 = \tau + 2. \quad (25)$$

It follows that only those sites of six-dimensional lattice, which are located at the distance not higher than $\tau + 2$ from the physical space, are projected within discussed model. Then, during the construction sites' groups of high orders, the density of its location will be limited due to finite size of projection region [21].

3. Quasi-Periodic Lattices with Octagonal Symmetry

Let show that algorithm $D_n = D_{n-1} + \{\tau^{n-2} \mathbf{q}_i\} D_{n-1}$ proposed for decagonal quasi-crystals is appropriate for using to quasi-crystalline lattices with octagonal symmetry.

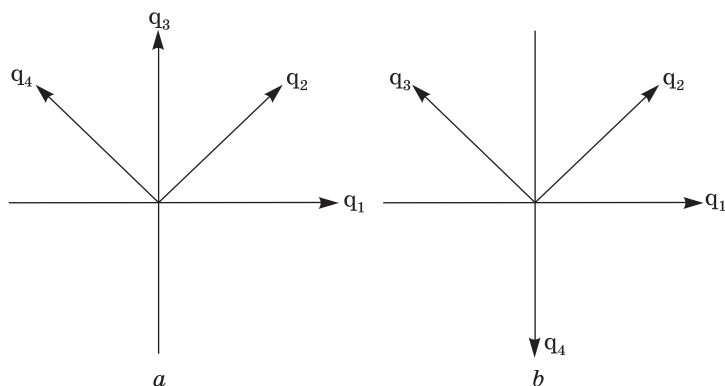


Fig. 8. Options for selection of the basis vectors for quasi-lattice, which possesses the octagonal symmetry

3.1. Real Space

The set of basis vectors has to be selected with two options, which are different in mutual orientation (Fig. 8):

$$\mathbf{q}_1 = (1\mathbf{i} + 0\mathbf{j}), \quad \mathbf{q}_2 = \left(\frac{\sqrt{2}}{2}(\mathbf{i} + \mathbf{j})\right), \quad \mathbf{q}_3 = (0\mathbf{i} + 1\mathbf{j}), \quad \mathbf{q}_4 = \left(-\frac{\sqrt{2}}{2}(\mathbf{i} - \mathbf{j})\right) \quad (26)$$

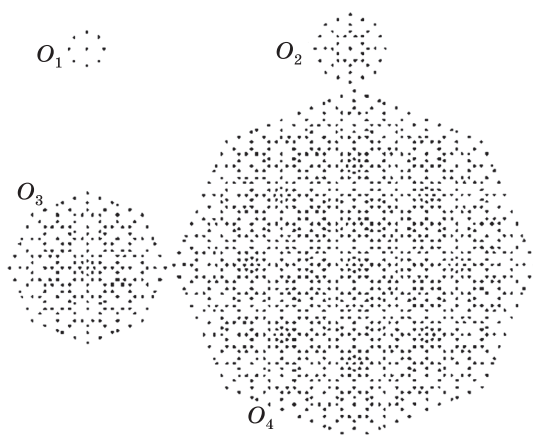
or

$$\mathbf{q}_1 = (1\mathbf{i} + 0\mathbf{j}), \quad \mathbf{q}_2 = \left(\frac{\sqrt{2}}{2}(\mathbf{i} + \mathbf{j})\right), \quad \mathbf{q}_3 = \left(-\frac{\sqrt{2}}{2}(\mathbf{i} - \mathbf{j})\right), \quad \mathbf{q}_4 = (0\mathbf{i} - 1\mathbf{j}). \quad (27)$$

As we can see, there is some ambiguity in selection of basis vectors. Then, if we consider \mathbf{q}_i as reciprocal lattice vectors, the ambiguity in indexing of diffraction reflexes of octagonal quasi-crystals will exist.

For example, let consider set (26) as the basis. Initial sites group O_1 is constructed with $(\pm\mathbf{q}_1, \pm\mathbf{q}_2, \pm\mathbf{q}_3, \pm\mathbf{q}_4)$ set of \mathbf{q}_i vectors. Algorithm for modelling the lattice can be expressed in the form

$$O_n = O_{n-1} + \{\delta_s^{n-2}\mathbf{q}_i\} O_{n-1}, \quad (28)$$



where we use 'silver ratio' ($\delta_s = 1 + \sqrt{2}$) as parameter by analogy with 'golden ratio' τ [28]. One of the properties of number δ_s is that exponent values for it can be expressed as

$$\delta_s^n = K_n \delta_s + K_{n-1}; \quad (29)$$

here, K_n are Pell's numbers (0; 1; 2; 5; 12; 29; 70; 169;

Fig. 9. Model for construction of the octagonal quasi-lattice

408; ...), which satisfy to $K_n = 2K_{n-1} + K_{n-2}$ condition [29]. It should be noted that there is a relation between the basis vectors:

$$\mathbf{q}_1 + \mathbf{q}_2 + \mathbf{q}_3 = \delta_s \mathbf{q}_2. \quad (30)$$

Then, using equations (29) and (30), we can write as following:

$$\begin{aligned} \delta_s^2 \mathbf{q}_2 &= 2(\mathbf{q}_1 + \mathbf{q}_2 + \mathbf{q}_3) + \mathbf{q}_2 = 2(\mathbf{q}_1 + \mathbf{q}_3) + 3\mathbf{q}_2; \\ \delta_s^3 \mathbf{q}_2 &= 5(\mathbf{q}_1 + \mathbf{q}_2 + \mathbf{q}_3) + 2\mathbf{q}_2 = 5(\mathbf{q}_1 + \mathbf{q}_3) + 7\mathbf{q}_2; \\ \delta_s^4 \mathbf{q}_2 &= 12(\mathbf{q}_1 + \mathbf{q}_2 + \mathbf{q}_3) + 5\mathbf{q}_2 = 12(\mathbf{q}_1 + \mathbf{q}_3) + 17\mathbf{q}_2; \\ &\dots \dots \dots \end{aligned} \quad (31)$$

$$\delta_s^n \mathbf{q}_2 = K_n(\mathbf{q}_1 + \mathbf{q}_2 + \mathbf{q}_3) + K_{n-1} \mathbf{q}_2 = K_n(\mathbf{q}_1 + \mathbf{q}_3) + (K_n + K_{n-1}) \mathbf{q}_2.$$

Thus, it is evidently that any site of $O_n = O_{n-1} + \{\delta_s^{n-2} \mathbf{q}_i\} O_{n-1}$ group can be expressed as linear combination of basis vectors in the form $\mathbf{Q} = n_1 \mathbf{q}_1 + n_2 \mathbf{q}_2 + n_3 \mathbf{q}_3 + n_4 \mathbf{q}_4$. Figure 9 illustrates the example of application of specified algorithm for O_4 sites group.

It is important that algorithm (28) can be modified by substitution of one or few numeral coefficients (Fig. 10):

- (a) $O_2 = O_1 + \{\mathbf{q}_i\} O_1, \dots, O_n = O_{n-1} + \{\delta_s^{n-2} \mathbf{q}_i\} O_{n-1};$
- (b) $O_2 = O_1 + \{\mathbf{q}_i\} O_1, O_3 = O_2 + \{2\mathbf{q}_i\} O_2, \dots, O_n = O_{n-1} + \{\delta_s^{n-3} \mathbf{q}_i\} O_{n-1};$
- (c) $O_2 = O_1 + \{\mathbf{q}_i\} O_1, O_3 = O_2 + \{\sqrt{2}\mathbf{q}_i\} O_2, \dots, O_n = O_{n-1} + \{\delta_s^{n-3} \mathbf{q}_i\} O_{n-1};$
- (d) $O_2 = O_1 + \{\sqrt{2}\mathbf{q}_i\} O_1, \dots, O_n = O_{n-1} + \{\delta_s^{n-2} \mathbf{q}_i\} O_{n-1}.$

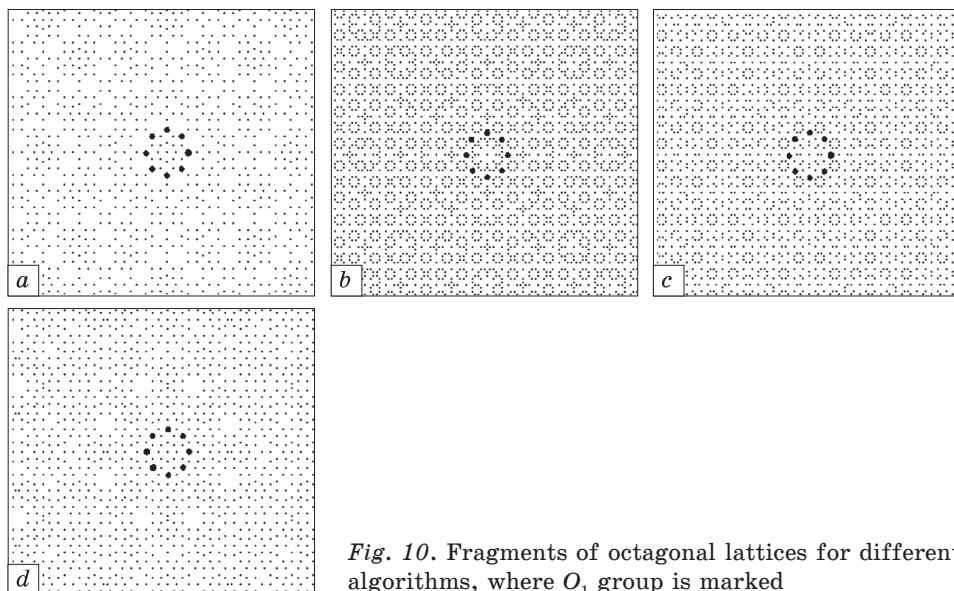


Fig. 10. Fragments of octagonal lattices for different algorithms, where O_1 group is marked

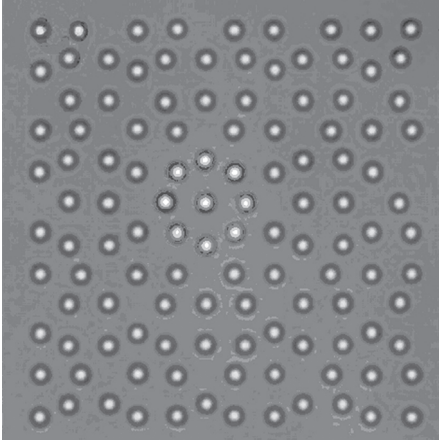


Fig. 11. Two-dimensional colloidal quasi-crystal [35]

Also momentous is condition that specified coefficients are expressed through relations between basis vectors similar to Eq. (30).

In contradistinction to known modelling methods [30–34], this proposed method for multiplying of sites groups allows to classify quasi-crystalline structures. For example, Fig. 11 illustrates two-dimensional quasi-periodic structure [35]. It is evident that this structure is in agreement with the model shown in Fig. 10, *d*. Such structure according to numeric coefficients in algorithm can be expressed as the structure of $O(\delta_s - 1, \delta_s^{n-2})$ type. The

structures obtained with other structure algorithms (Fig. 10, *a*, *b*, *c*) can be denoted as $O(1, \delta_s^{n-2})$, $O(1, 2, \delta_s^{n-3})$ and $O(1, \delta_s - 1, \delta_s^{n-2})$, respectively. It is easy to show that variation of algorithm consists in rearrangement of coefficients at \mathbf{q}_i . For instance, $O_2 = O_1 + \{\delta_s \mathbf{q}_i\} O_1$, $O_3 = O_2 + \{\mathbf{q}_i\} O_2$, $O_4 = O_3 + \{2\mathbf{q}_i\} O_3$, ..., $O_n = O_{n-1} + \{\delta_s^{n-3} \mathbf{q}_i\} O_{n-1}$ leads to construction the structure, which is the same as obtained with $O_2 = O_1 + \{\mathbf{q}_i\} O_1$, $O_3 = O_2 + \{2\mathbf{q}_i\} O_2$, ..., $O_n = O_{n-1} + \{\delta_s^{n-3} \mathbf{q}_i\} O_{n-1}$. That is why it is advisable to note the coefficients in notation of structural class in ascending order.

It is known [36, 37] that quasi-crystalline lattice can be represented as projection of periodic lattice in the space with dimensionality R onto space with dimensionality d . In the case of octagonal plain quasi-lattice, it can be proposed the projection of four-dimensional hyper-cubic lattice onto the plain. If the basis of four-dimensional lattice are represented as orthogonal vectors,

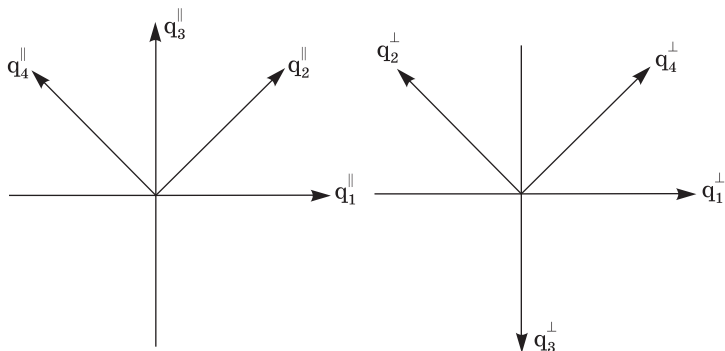
$$\begin{aligned} \mathbf{u}_1 &= [1 \ 0 \ 1 \ 0], & \mathbf{u}_2 &= [\sqrt{2}/2 \ \sqrt{2}/2 \ -\sqrt{2}/2 \ \sqrt{2}/2], \\ \mathbf{u}_3 &= [0 \ 1 \ 0 \ -1], & \mathbf{u}_4 &= [-\sqrt{2}/2 \ \sqrt{2}/2 \ \sqrt{2}/2 \ \sqrt{2}/2], \end{aligned} \quad (32)$$

then, the first two coordinates of each vector correspond to basis vectors. Two of rest coordinates correspond to the vectors

$$\begin{aligned} \mathbf{q}_1^\perp &= (\mathbf{i} + 0\mathbf{j}), & \mathbf{q}_2^\perp &= (-\sqrt{2}/2)\mathbf{i} + (\sqrt{2}/2)\mathbf{j}, \\ \mathbf{q}_3^\perp &= (0\mathbf{i} - 1\mathbf{j}), & \mathbf{q}_4^\perp &= ((\sqrt{2}/2)\mathbf{i} + (\sqrt{2}/2)\mathbf{j}), \end{aligned} \quad (33)$$

which are projection of set (32) onto ‘perpendicular’ space. Mutual orientation of basis vectors in ‘perpendicular’ space with preset basis in

Fig. 12. Mutual orientation of basis vectors (32) at their projection to physical and 'perpendicular' spaces



physical space is presented in Fig. 12. Evidently, the vector of physical space $\mathbf{q}_1 + \mathbf{q}_2 + \mathbf{q}_3$ corresponds to the vector of 'perpendicular' space $\mathbf{q}_1^\perp + \mathbf{q}_2^\perp + \mathbf{q}_3^\perp$, whose modulus has a minimal value for all combinations of three basis vectors.

We show that algorithm (28) corresponds to the sites of four-dimensional hyper-cubic lattice, which are closely located to physical space. By this way, it will prove that proposed method and projected method are equivalent between each other. For this, it is enough to show that 'the radius' of sites group in 'perpendicular' space (maximal distance from sites of four-dimensional space to physical space) is finite. As seen from Fig. 12, the next equation is valid during execution of Eq. (30):

$$\mathbf{q}_1^\perp + \mathbf{q}_2^\perp + \mathbf{q}_3^\perp = -(\sqrt{2} - 1)\mathbf{q}_2^\perp = -(1/\delta_s)\mathbf{q}_2^\perp. \quad (34)$$

We can show from Eqs. (31) and (34) that boundary radii of sites' groups $r_{n \rightarrow \infty}$ and $r_{n \rightarrow \infty}^\perp$ are equal to

$$r_{n \rightarrow \infty} = 1 + \sum_{n=2}^{\infty} \delta_s^{n-2} = \infty,$$

$$r_{n \rightarrow \infty}^\perp = 1 + \sum_{n=2}^{\infty} \delta_s^{2-n} = 1 + \frac{1}{1 - \delta_s^{-1}} = 1 + \frac{\delta_s + 1}{2} = 2 + \frac{\sqrt{2}}{2}.$$

Thus, the distance from projected four-dimensional lattice to physical space does not exceed $2 + \sqrt{2}/2$. Hence, proposed method is quite correct.

3.2. Reciprocal Octagonal Lattice

Let us analyse the possibility of using the proposed model for reciprocal lattice of the octagonal quasi-crystals.

We can reduce the square values of modules of vectors $\mathbf{Q}_\parallel = n_1\mathbf{q}_1 + n_2\mathbf{q}_2 + n_3\mathbf{q}_3 + n_4\mathbf{q}_4$, $\mathbf{Q}_\perp = n_1\mathbf{q}_1^\perp + n_2\mathbf{q}_2^\perp + n_3\mathbf{q}_3^\perp + n_4\mathbf{q}_4^\perp$, and $\mathbf{Q} = n_1\mathbf{u}_1 + n_2\mathbf{u}_2 + n_3\mathbf{u}_3 + n_4\mathbf{u}_4$ (in physical, 'perpendicular', and four-dimensional spaces, respectively) to the form:

$$|\mathbf{Q}_\parallel|^2 = (n_1^2 + n_2^2 + n_3^2 + n_4^2) + (n_1n_2 + n_2n_3 + n_3n_4 - n_1n_4)\sqrt{2},$$

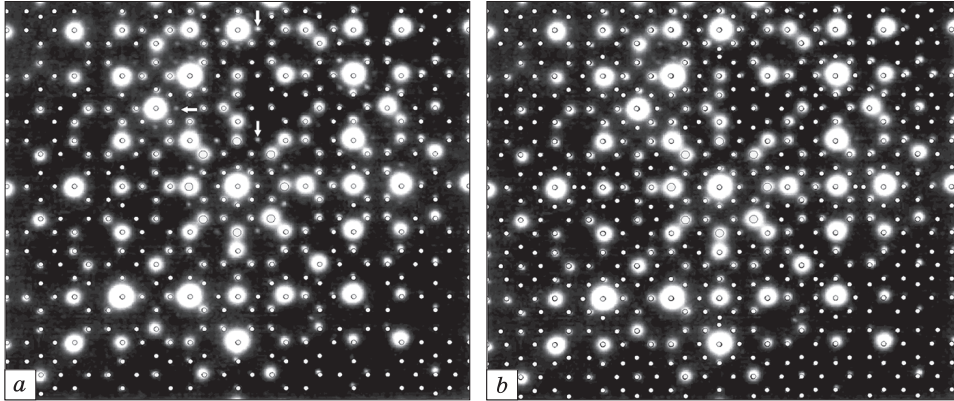


Fig. 13. The overlap of the groups of O_4 sites on electron diffraction pattern from octagonal quasi-crystal of the $Mn_4(Al,Si)$ system oriented by its symmetry axis of the 8-th order along the electron beam (diffraction pattern adopted from paper [38])

$$|\mathbf{Q}_\perp|^2 = (n_1^2 + n_2^2 + n_3^2 + n_4^2) - (n_1n_2 + n_2n_3 + n_3n_4 - n_1n_4)\sqrt{2}, \quad (35)$$

$$|\mathbf{Q}|^2 = |\mathbf{Q}_\perp|^2 + |\mathbf{Q}_\parallel|^2 = 2(n_1^2 + n_2^2 + n_3^2 + n_4^2).$$

Using denotations

$$\begin{aligned} N &= (n_1^2 + n_2^2 + n_3^2 + n_4^2) - (n_1n_2 + n_2n_3 + n_3n_4 - n_1n_4), \\ M &= (n_1n_2 + n_2n_3 + n_3n_4 - n_1n_4), \end{aligned} \quad (36)$$

we can deduce

$$|\mathbf{Q}_\parallel|^2 = N + M\delta_s \quad (37)$$

that has similar form to equations for icosahedral (1) quasi-crystals [1] as well as for plain lattice of decagonal (5) quasi-crystals [21]. At the same time, the squared distance from site of four-dimensional lattice to its corresponding projection in physical space is defined by $N\delta_s - M$ value:

$$|\mathbf{Q}_\perp|^2 = (N\delta_s - M)/\delta_s. \quad (38)$$

According to Refs. [18, 20, 34, 36], the value of $|\mathbf{Q}_\perp|^2$ defines the intensity of diffraction reflexes. It is important that $|\mathbf{Q}_\perp|^2 \propto (N\tau - M)$ for the icosahedral and decagonal lattices.

The translation of O_{n-1} sites' groups on $\delta_s^{n-2}\mathbf{q}_i$ value corresponds to shifting its centres to positions of $(n_1n_2n_3n_4)$ sites of the (1110)-, (2320)-, (5750)-, (1217120)-, ..., $(K_n, K_n + K_{n-1}, K_n, 0)$ -type according to Eqs. (29) and (30). The substitution of these indices in Eq. (36) gives the pairs of values $N = K_n^2 + K_{n-1}^2$ and $M = 2(K_n^2 + K_nK_{n-1})$: (1, 2); (5, 12); (29, 70); (169, 408); ... Thus, squared modulus values for shifting vectors of sites groups can be expressed throw the pairs of N and M numbers, which are neighbouring elements in Pell's sequence. The corresponding pairs of numbers satisfy to the condition $M/N < \delta_s$, which is necessary

condition according to Eq. (38). It is can be verified that the value of $|\mathbf{Q}_\perp|^2$ defined from Eq. (38) is small for these numbers' pairs as compared to any other numbers' pairs.

Table 3. Characteristics of some sites of O_7 groups constructed according to algorithms (28) and (39)

No.	$(n_1 \ n_2 \ n_3 \ n_4)$	N	M	$ \mathbf{Q}_\perp ^2$	Quantity of overlaps (28)	Quantity of overlaps (39)
1	(1 -1 1 0)	5	-2	5.828	5	78
2	(-1 2 -1 0)	10	-4	11.657		11
3	(0 0 1 -1)	3	-1	3.414	12	108
4	(1 0 0 0)	1	0	1	43	223
5	(1 1 -1 1)	6	-2	6.828		48
6	(-1 1 1 -2)	11	-4	12.657		12
7	(2 -1 1 0)	9	-3	10.243		22
8	(0 2 -1 0)	7	-2	7.828		46
9	(0 0 2 -2)	12	-4	13.657		6
10	(1 0 1 0)	2	0	2	26	170
11	(1 0 1 -1)	3	0	3	25	150
12	(1 1 0 0)	1	1	0.586	48	224
13	(2 0 0 0)	4	0	4	14	119
14	(0 1 1 -2)	7	-1	7.414		54
15	(2 0 1 0)	5	0	5	10	96
16	(1 1 1 0)	1	2	0.172	73	257
17	(2 1 0 1)	6	0	6	4	78
18	(1 1 1 -1)	2	2	1.172	52	236
19	(0 2 1 -1)	5	1	4.586	16	112
20	(2 1 0 0)	3	2	2.172	28	162
21	(1 1 2 -1)	5	2	4.172	15	110
22	(2 1 1 0)	3	3	1.756	42	222
23	(1 2 1 0)	2	4	0.343	78	286
24	(2 2 -1 0)	7	2	6.172		61
25	(1 2 1 -1)	3	4	1.343	44	196
26	(2 2 0 0)	4	4	2.343	32	202
27	(1 3 0 0)	7	3	5.757	8	96
28	(2 1 2 0)	5	4	3.343	17	131
29	(2 1 2 -1)	6	4	4.343	20	131
30	(3 1 1 0)	7	4	5.343	5	81
31	(1 2 2 -1)	5	5	2.929	32	192
32	(2 2 1 0)	3	6	0.515	48	213
33	(1 3 1 0)	5	6	2.515	27	151
34	(2 2 1 -1)	3	7	0.101	104	332
35	(1 3 1 -1)	6	6	3.515	32	172
36	(2 3 0 0)	7	6	4.515	7	89
37	(2 2 2 0)	4	8	0.686	54	276
38	(3 1 2 -1)	9	6	6.515	3	63

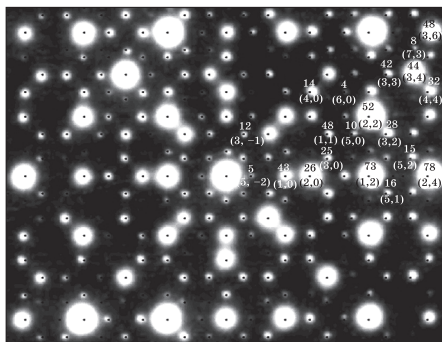


Fig. 14. Indices (N, M) and the quantity of site overlaps (algorithm (28), O_7 group) for the corresponding reflex on electron diffraction pattern adopted from Ref. [38]

Figure 13, *a* illustrates the overlapping of O_4 sites group on the electron diffraction pattern for octagonal quasi-crystal of $Mn_4(Al, Si)$ system. Evidently, the sites of constructed lattice totally coincide with

reflexes from diffraction pattern. Therewith, there are reflexes with low intensities, which have no corresponding site on the model (some of them are marked with the point in Fig. 13). Changing algorithm for construction of $O_2 = O_1 + \{\mathbf{q}_i\}O_1$ into $O_2 = O_1 + \{\sqrt{2}\mathbf{q}_i\}O_1$ (the next steps of algorithm remain unchanged) causes the appearance of additional sites, which coincide with marked reflexes (Fig. 13, *b*). Thus, diffraction pattern for octagonal quasi-crystal $Mn_4(Al, Si)$ is related to $O(\delta_s - 1, \delta_s^{n-2})$, class by geometry. Such algorithm change corresponds to extending of projection region in four-dimensional space, because $r_{n \rightarrow \infty}^\perp = 2 + \sqrt{2}/2 + (\sqrt{2} - 1)$ in this case.

Table 3 presents the characteristics of some reciprocal lattice sites, which are the most closely located to coordinate start. These sites have been generated according to algorithms (28) and the following relationship:

$$O_n = O_{n-1} + \{\delta_s^{n-3}\mathbf{q}_i\}O_{n-1}. \quad (39)$$

As a result of construction of the octagonal quasi-lattices, using described algorithms (as well as in the case of the construction of decagonal quasi-lattices), there is a multiple mutual overlapping of the sites. The quantity of this overlaps for various algorithms is presented in the last two columns of Table 3. As shown, the correlation between overlapping quantity and $|\mathbf{Q}_\perp|^2$ value is observed for all proposed algorithms as well as for decagonal quasi-lattice (Table 2).

Figure 14 shows indices and the quantity of overlaps (algorithm (28)) for appropriate reflexes on electron diffraction pattern for octagonal quasi-crystal of $Mn_4(Al, Si)$ system. As seen, the quantity of overlaps is in a distinct agreement with intensity of diffraction reflexes.

Reflexes with the next values of indices (N, M) should have sufficiently high intensity according to obtained results:

$$(1,0); (2,0); (1,1); (1,2); (2,4); (3,4); (3,6); (3,7); (4,8); (5,1); \dots \quad (40)$$

Reasoning from the three-dimensionality of octagonal quasi-crystals and its periodicity along 8th-order symmetry axis, inter-planar distanc-

es can be calculated by the equation, which is similar to obtained one for decagonal quasi-crystals (19):

$$1/d^2 = (N + M\delta_s)/a^2 + L^2/c^2; \quad (41)$$

here, a is spacing parameter of plain quasi-lattice, c is spacing parameter along 8th-order symmetry axis.

In practice, value of L index does not exceed 2 during indexing of XRD (x-ray diffraction) patterns. That is why the number of possible combinations of three indices (N, M, L) is rather small. It should be noted that reflexes of $(0, 0, L)$ -type can also be observed on diffraction patterns in addition to reflexes of (N, M, L) -type (with N and M indices, which correspond to values of Eq. (40)). Therefore, the indexing of XRD-patterns for octagonal quasi-crystals should be considered as similar to indexing of crystalline materials, which belong to middle crystals' systems.

4. Dodecagonal Quasi-Periodic Lattices

The formation of condensed matter with quasi-periodic long-range order and with the 12th-order symmetry axis has been established not only for metal systems (as like Ni–V [39], Cr–Ni [40], Bi–Mn [41], Ta–Te [42], and Mn–Si–V [43]), but also for liquid crystals [44], colloidal solutions [45], and polymer systems [46].

Interpretation of the electron and x-ray diffraction patterns for dodecagonal quasi-crystals, as well as for all others, is also ambiguous because of indetermination of indexing of diffraction reflections. Such ambiguity is caused by inflation–deflation symmetry, which is native for quasi-crystals. As a result, the ratio of the absolute values of the reciprocal lattice vectors is expressed in terms of so-called scaling factor [20–23]. In electron diffraction studies of quasi-crystals, basis vectors are commonly match with reflections closest to the trace of the primary beam, which have a very low intensity, as a rule. For this reason, the minimal (basis) reciprocal lattice vectors (determined in diffraction experiments) are dependent on the experimental conditions.

For construction of two-dimensional reciprocal quasi-lattice, let use algorithm in the form of recurrent equation:

$$D_n = D_{n-1} + \{k^{n-2}\mathbf{q}_i\} D_{n-1}. \quad (42)$$

In this case, the k parameter (for dodecagonal lattice, let us denote it as t) was chosen from geometric interpretation of τ and δ_s numbers and from the condition that this numbers belong to Pisot numbers [5, 31, 34, 47] $\tau = 2\cos(2\pi/10)$ and $\delta_s = 1 + 2\cos(2\pi/8)$:

$$k = t = 1 + 2\cos(2\pi/12), \quad (43)$$

$$k = t_1 = 2 + 2\cos(2\pi/12). \quad (44)$$

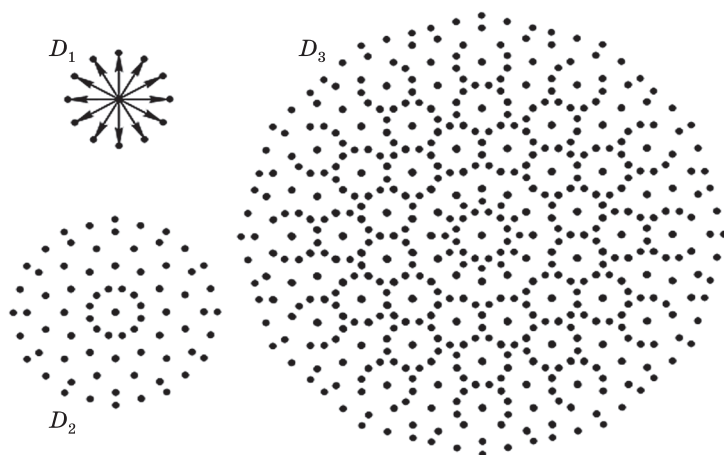


Fig. 15. Groups of sites obtained according to algorithm (42) and parameter (43) (D_1 is an initial group of sites)

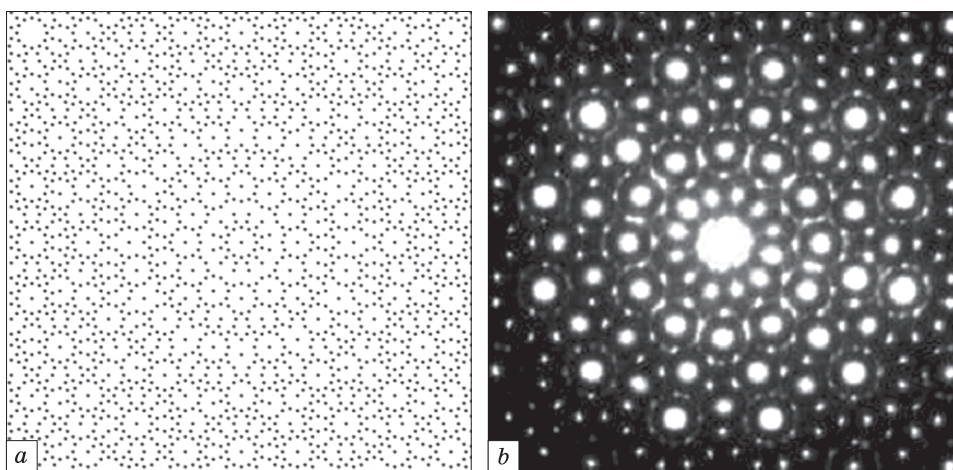
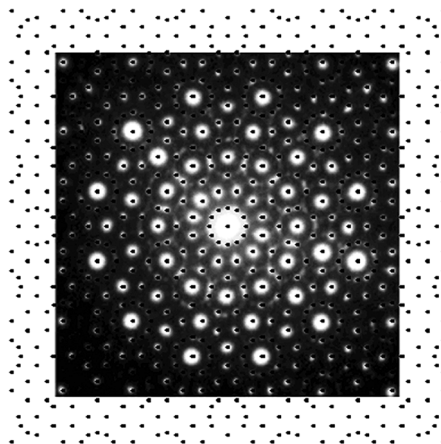


Fig. 16. Comparison of fragment of group D_5 sites (a) (algorithm (42) and parameter (44)) with electron diffraction pattern from dodecagonal quasi-crystal (b) of Ta–Te system obtained in Ref. [49]

Parameters (43) and (44) have been used as scaling factors for a dodecagonal lattice in papers [5, 31, 48].

As shown earlier, the application of algorithm (42) for the octagonal and decagonal quasi-crystals results to complete agreement between obtained quasi-lattices and experimental electron diffraction patterns. The implementation of algorithm (43) and (44) is illustrated in Fig. 15. The comparison of this lattice with the electron diffraction pattern of a dodecagonal quasi-crystal (Fig. 16) [26] shows the qualitative conformity between them.

Fig. 17. The overlap of group D_5 (algorithm (45)) on the electron diffraction pattern [49] from quasi-crystal of Ta-Te system



The usage of parameter (44) for the implementation of algorithm (42) leads to discontinuities of the lattice. The conformity of the model quasi-lattice with above-specified electron diffraction is observed after the replacement of algorithm (1) with the algorithm proposed earlier in Ref. [27], which can be written in the form of the following recurrent relations (Fig. 17):

$$\begin{aligned} D_2 &= D_1 + \{\mathbf{q}_i\} D_1, \quad D_3 = D_2 + \{2\mathbf{q}_i\} D_2, \quad D_4 = D_3 + \{t_1 \mathbf{q}_i\} D_3, \\ D_5 &= D_4 + \{2t_1 \mathbf{q}_i\} D_4, \quad D_6 = D_5 + \{t_1^2 \mathbf{q}_i\} D_5, \quad D_7 = D_6 + \{2t_1^2 \mathbf{q}_i\} D_6. \end{aligned} \quad (45)$$

The numbers t and t_1 are the solutions for quadratic equations $x_2 = 2x + 2$ and $x_2 = 4x - 1$, respectively. It follows, hence, that any power of t and t_1 can be expressed in terms of these numbers proper (e.g., $t^3 = 6t + 4$, $t^4 = 16t + 12$, ... ; $t_1^3 = 15t - 4$, $t_1^4 = 56t - 15$, ...). We must take into account that basis vectors \mathbf{q}_i of a dodecagonal lattice relate as $\mathbf{q}_1 + \mathbf{q}_2 + \mathbf{q}_3 = t\mathbf{q}_2$ and $\mathbf{q}_1 + 2\mathbf{q}_2 + \mathbf{q}_3 = t_1\mathbf{q}_2$. Therefore, one can easily see that the positions of all sites appearing in the realization of the above algorithms can be expressed in terms of a linear combination of \mathbf{q}_i vectors. Thus, each site of model quasi-lattices can be indexed.

Let us compare the proposed method of recurrent multiplication of site groups with the projecting method. Since six basis vectors are used for a 2D-dodecagonal lattice, it is logically to use a six-dimensional hyper-cubic lattice. We require that the first two components of the coordinates of six-dimensional basis vectors represent the basis coordinates of a 2D-dodecagonal quasi-lattice. Then, we can use the unit orthogonal basis vectors proposed in paper [31],

$$\begin{aligned} \mathbf{u}_1 &= (1, 0, 1, 0, 1/\sqrt{2}, 1/\sqrt{2})/\sqrt{3}, \\ \mathbf{u}_2 &= (\sqrt{3}/2, 1/2, -\sqrt{3}/2, 1/2, -1/\sqrt{2}, 1/\sqrt{2})/\sqrt{3}, \\ \mathbf{u}_3 &= (-1/2, -\sqrt{3}/2, -1/2, \sqrt{3}/2, 1/\sqrt{2}, 1/\sqrt{2})/\sqrt{3}, \\ \mathbf{u}_4 &= (0, -1, 0, -1, -1/\sqrt{2}, 1/\sqrt{2})/\sqrt{3}, \\ \mathbf{u}_5 &= (-1/2, \sqrt{3}/2, -1/2, -\sqrt{3}/2, 1/\sqrt{2}, 1/\sqrt{2})/\sqrt{3}, \\ \mathbf{u}_6 &= (-\sqrt{3}/2, 1/2, \sqrt{3}/2, 1/2, -1/\sqrt{2}, 1/\sqrt{2})/\sqrt{3}, \end{aligned} \quad (46)$$

or suggest another set of vectors:

$$\begin{aligned}
 \mathbf{u}_1 &= (1, 0, 1, 0, 1, 0)/\sqrt{3}, \\
 \mathbf{u}_2 &= (\sqrt{3}/2, 1/2, -\sqrt{3}/2, -1/2, 0, 1)/\sqrt{3}, \\
 \mathbf{u}_3 &= (1/2, \sqrt{3}/2, 1/2, \sqrt{3}/2, -1, 0)/\sqrt{3}, \\
 \mathbf{u}_4 &= (0, 1, 0, -1, 0, -1)/\sqrt{3}, \\
 \mathbf{u}_5 &= (-1/2, \sqrt{3}/2, -1/2, \sqrt{3}/2, 1, 0)/\sqrt{3}, \\
 \mathbf{u}_6 &= (-\sqrt{3}/2, 1/2, \sqrt{3}/2, -1/2, 0, 1)/\sqrt{3}.
 \end{aligned} \tag{47}$$

Each vector in Eq. (46) or (47) has two components corresponding to the two-dimensional physical (*i.e.*, real) space and two components corresponding to the ‘perpendicular’ space. Therefore, we can write these vectors as $\mathbf{u}_i = (\mathbf{q}_i^{\parallel}; \mathbf{q}_i^{\perp})$. For each site in the physical space, to correspond uniquely to a vector in the ‘perpendicular’ space, it is necessary that, for the linear combination of vectors that gives a zero vector (*e.g.*, $\mathbf{q}_1^{\parallel} - \mathbf{q}_3^{\parallel} + \mathbf{q}_5^{\parallel} = 0$ and $\mathbf{q}_2^{\parallel} - \mathbf{q}_4^{\parallel} + \mathbf{q}_6^{\parallel} = 0$ for vectors (48) given below), the corresponding combination of vectors \mathbf{q}_i^{\perp} can be also equal to zero. As revealed, vectors (46) and (47) do not satisfy this requirement. Then, as the basis, we can choose vectors obtained from set (47) in the following manner:

$$\begin{aligned}
 \mathbf{u}_1^* &= (\mathbf{u}_2 - \mathbf{u}_6) = (1, 0, -1, 0, 0, 0), \\
 \mathbf{u}_2^* &= (\mathbf{u}_1 + \mathbf{u}_3) = (\sqrt{3}/2, 1/2, \sqrt{3}/2, 1/2, 0, 0), \\
 \mathbf{u}_3^* &= (\mathbf{u}_2 + \mathbf{u}_4) = (1/2, \sqrt{3}/2, -1/2, -\sqrt{3}/2, 0, 0), \\
 \mathbf{u}_4^* &= (\mathbf{u}_3 + \mathbf{u}_5) = (0, 1, 0, 1, 0, 0), \\
 \mathbf{u}_5^* &= (\mathbf{u}_4 + \mathbf{u}_6) = (-1/2, \sqrt{3}/2, 1/2, -\sqrt{3}/2, 0, 0), \\
 \mathbf{u}_6^* &= (\mathbf{u}_5 - \mathbf{u}_1) = (-\sqrt{3}/2, 1/2, -\sqrt{3}/2, 1/2, 0, 0).
 \end{aligned} \tag{48}$$

Omitting in these expressions (48) the last two coordinates, we can obtain the four-dimensional non-orthogonal basis of the lattice, which is

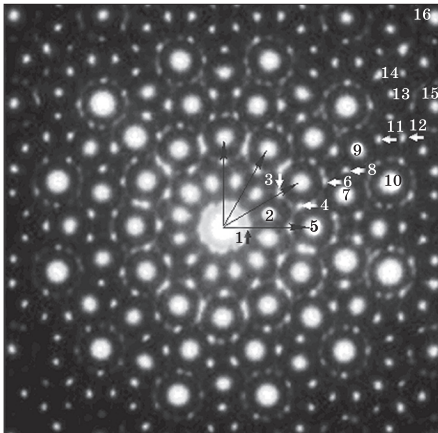


Fig. 18. Reflexes of electron diffraction pattern [49] corresponding to basis vectors according to the algorithm (45) (numbered reflexes are described in Table 4)

Table 4. Indices and characteristics of the sites indicated in Fig. 18

No.	$(n_1 \ n_2 \ n_3 \ n_4)$	$N^*; M^*$	$N; M$	$N_1; M_1$	$ \mathbf{Q} ^2$	$ \mathbf{Q}_\perp ^2$	Quantity of site self-overlaps
1	(2 -2 0 1)	7; -4	11; -4	15; -4	0.072	13.928	37
2	(1 0 -1 1)	2; -1	3; -1	4; -1	0.268	3.732	182
3	(1 -1 1 0)	4; -2	6; -2	8; -2	0.536	7.464	118
4	(-1 1 2 -2)	6; -3	9; -3	12; -3	0.804	11.196	76
5	(1 0 0 0)	1; 0	1; 0	1; 0	1	1	245
6	(2 -1 0 1)	5; -2	7; -2	9; -2	1.536	8.464	144
7	(0 1 1 -1)	2; 0	2; 0	2; 0	2	2	266
8	(1 1 -1 1)	4; -1	5; -1	6; -1	2.268	5.732	194
9	(1 0 1 0)	3; 0	3; 0	3; 0	3	3	350
10	(1 1 0 0)	2; 1	1; 1	0; 1	3.732	0.268	326
11	(0 2 0 0)	4; 0	4; 0	4; 0	4	4	335
12	(2 0 0 1)	5; 0	5; 0	5; 0	5	5	328
13	(1 1 0 1)	4; 1	3; 1	2; 1	5.732	2.268	346
14	(-1 2 2 -1)	6; 0	6; 0	6; 0	6	6	292
15	(1 1 1 0)	4; 2	3; 2	1; 2	7.464	0.536	387
16	(1 1 1 1)	6; 3	3; 3	0; 3	11.196	0.804	440

analogous to the basis proposed in Ref. [31]. It can be verified that the reciprocal angles between the triples of four-dimensional vectors (\mathbf{u}_1^* , \mathbf{u}_3^* , \mathbf{u}_5^*) and (\mathbf{u}_2^* , \mathbf{u}_4^* , \mathbf{u}_6^*) are equal to 60° and 120° . At the same time, each vector from a triple is orthogonal to vectors from another set. It follows, hence, that we can consider the given four-dimensional lattice as a combination of two 2D hexagonal sublattices, the spaces of which are mutually orthogonal. According to Ref. [50], such a lattice belongs to a bi-isohexagonal orthogonal system. In the given basis, only four vectors are linearly independent. Therefore, two vectors (e.g., \mathbf{u}_5^* and \mathbf{u}_6^*) can be omitted, writing the basis of the 4D lattice in the form:

$$\begin{aligned} \mathbf{q}_1^* &= (1, 0, -1, 0); & \mathbf{q}_2^* &= (\sqrt{3}/2, 1/2, \sqrt{3}/2, 1/2); \\ \mathbf{q}_3^* &= (1/2, \sqrt{3}/2, -1/2, -\sqrt{3}/2); & \mathbf{q}_4^* &= (0, 1, 0, 1). \end{aligned} \quad (49)$$

Evidently, if we put vectors (49) in correspondence to the basis group of sites in the proposed model, the sites generated in accordance with algorithm (45) will be projections of certain sites in the indicated four-dimensional lattice.

It is easy to see that, in both cases of the octagonal and dodecagonal lattices during the multiplication of sites of a dodecagonal lattice in accordance with algorithm (45), a correlation between the number of self-overlaps of sites and the intensity of the corresponding diffraction reflections is also observed (Fig. 18, Table 4).

Let us put in correspondence the intensities of reflections to the distance from the sites of a $4D$ lattice to the physical space. Each site of this lattice can be represented as $\mathbf{Q} = (\mathbf{Q}^{\parallel}; \mathbf{Q}^{\perp})$, where

$$\mathbf{Q}^{\parallel} = \sum_1^4 n_i \mathbf{q}_i^{\parallel} \text{ and } \mathbf{Q}^{\perp} = \sum_1^4 n_i \mathbf{q}_i^{\perp}. \quad (50)$$

Then, squared values of vectors \mathbf{Q}^{\parallel} and \mathbf{Q}^{\perp} are as follow:

$$|\mathbf{Q}^{\parallel}|^2 = \left(\sum_1^4 n_i^2 + n_1 n_3 + n_2 n_4 \right) + (n_1 n_2 + n_2 n_3 + n_3 n_4) \sqrt{3} = N^* + M^* \sqrt{3}, \quad (51)$$

$$|\mathbf{Q}^{\perp}|^2 = \left(\sum_1^4 n_i^2 + n_1 n_3 + n_2 n_4 \right) - (n_1 n_2 + n_2 n_3 + n_3 n_4) \sqrt{3} = N^* - M^* \sqrt{3}. \quad (52)$$

The calculation of $|\mathbf{Q}^{\perp}|$ value is based on Eq. (52) for reflections in Fig. 18 shows that a correlation is observed between $|\mathbf{Q}^{\perp}|$, the number of self-overlaps of sites in the modelling, and the intensity of reflections (Table 1).

The equation for calculation of $|\mathbf{Q}^{\parallel}|$ in both cases of using t and t_1 parameters can be reduced to the form similar to Eqs. (5) and (37):

$$|\mathbf{Q}^{\parallel}|^2 = N + Mt, \quad |\mathbf{Q}^{\parallel}|^2 = N_1 + M_1 t_1; \quad (53)$$

here, $N = N^* - M^*$, $M = M^*$, $N_1 = N^* - 2M^*$, $M_1 = M^*$. Within the value of $|\mathbf{Q}^{\perp}|$ (in contrast of to those of icosahedral, octagonal, and dodecagonal

Table 5. Indices of the sites (Fig. 18) with basis vectors corresponding to the reflexes located near the central spot

No.	$(n_1 \ n_2 \ n_3 \ n_4)_{\text{ch}}$	$N_{\text{ch}}; M_{\text{ch}}$	$ \mathbf{Q}^{\parallel} ^2$	$ \mathbf{Q}^{\perp} ^2$
1	(1 0 0 0)	1; 0	1	1
2	(1 1 0 0)	2; 1	3.732	0.268
3	(1 1 1 0)	4; 2	7.464	0.536
4	(1 2 1 -1)	6; 3	11.196	0.804
5	(2 2 0 -1)	7; 4	13.928	0.072
6	(2 2 1 0)	11; 6	21.392	0.608
7	(2 3 1 -1)	14; 8	27.856	0.144
8	(2 3 1 0)	16; 9	31.588	0.412
9	(2 3 2 0)	21; 12	41.785	0.215
10	(3 4 1 -1)	26; 15	51.981	0.019
11	(2 4 2 0)	28; 16	55.713	0.287
12	(3 4 2 0)	35; 20	69.641	0.359
13	(2 4 3 1)	40; 23	79.837	0.163
14	(1 4 4 1)	42; 24	83.569	0.431
15	(3 5 3 0)	52; 30	103.96	0.038
16	(2 5 5 2)	78; 45	155.94	0.058

quasi-lattices) cannot be reduced to the form $|\mathbf{Q}^\perp|^2 \propto (Nk - M)$:

$$|\mathbf{Q}^\perp| = N - 2M/t, \quad |\mathbf{Q}^\perp| = N_1 + M_1/t_1. \quad (54)$$

Basis vectors of reciprocal lattice are ascribed in [48] to low-intensity reflections that are closest to the trace of primary beam. In this case, the indices of the reflections and the magnitudes of corresponding vectors are recalculated by the following formulas:

$$N_{\text{ch}} = 7N^* + 12M^*, \quad M_{\text{ch}} = 4N^* + 7M^*, \quad (55)$$

$$|\mathbf{Q}_{\text{ch}}^\parallel|^2 = \frac{|\mathbf{Q}^\parallel|^2}{7 - 4\sqrt{3}} = |\mathbf{Q}^\parallel|^2 (7 + 4\sqrt{3}), \quad |\mathbf{Q}_{\text{ch}}^\perp|^2 = \frac{|\mathbf{Q}^\perp|^2}{7 + 4\sqrt{3}} = |\mathbf{Q}^\perp|^2 (7 - 4\sqrt{3}).$$

The results of calculations for characteristics of reflexes (Fig. 18) obtained with Eq. (55) are presented in Table 5.

Note that, with such indexing of intense reflections, the rounding of $M_{\text{ch}}\sqrt{3}$ value to the larger integer yields the value of N_{ch} . The values of $|\mathbf{Q}_{\text{ch}}^\parallel|^2$ and $|\mathbf{Q}_{\text{ch}}^\perp|^2$ are also determined only by M_{ch} value, *i.e.*,

$$N_{\text{ch}} = [M_{\text{ch}}\sqrt{3} + 1], \quad (56)$$

$$|\mathbf{Q}_{\text{ch}}^\parallel|^2 = [M_{\text{ch}}\sqrt{3} + 1] + M_{\text{ch}}\sqrt{3}, \quad |\mathbf{Q}_{\text{ch}}^\perp|^2 = [M_{\text{ch}}\sqrt{3} + 1] - M_{\text{ch}}\sqrt{3}.$$

According to [51, 52], low-intensive reflections in the vicinity of central spot on electron diffraction patterns are the results of multiple diffraction typical of quasi-crystals. At the same time, many authors take these reflections as those corresponding to basis vectors [48, 49]. In our model, the basis vectors of the reciprocal lattice correspond to reflections of type 5 (Fig. 18), which is in agreement with the results obtained in [51, 52]. Therefore, the proposed model of recurrent multiplication of site groups takes into account the effect of multiple diffraction and, at the same time, correctly maps the basis vectors on the diffraction pattern. The existence of correlation between the quantity of self-overlaps of sites and the intensity of diffraction reflections indicates that the procedure of recurrent construction of site groups is a certain analog of multiple diffraction processes.

To pass from the reciprocal space to the real one, we write vectors (49) as $\mathbf{a}_i^* = a_{4D}^* \mathbf{q}_i^* / \sqrt{2}$ where a_{4D}^* is a space parameter of four-dimensional reciprocal lattice. Using the condition $\mathbf{a}_i^* \mathbf{a}_j = \delta_{ij}$, we can define the basis vectors of the direct lattice as follows

$$\mathbf{a}_1 = \frac{a_{4D}}{\sqrt{2}} (\sqrt{3}/2, -1/2, -\sqrt{3}/2, 1/2), \quad \mathbf{a}_2 = \frac{a_{4D}}{\sqrt{2}} (1, 0, 1, 0), \quad (57)$$

$$\mathbf{a}_3 = \frac{a_{4D}}{\sqrt{2}} (0, 1, 0, -1), \quad \mathbf{a}_4 = \frac{a_{4D}}{\sqrt{2}} (-1/2, \sqrt{3}/2, -1/2, \sqrt{3}/2);$$

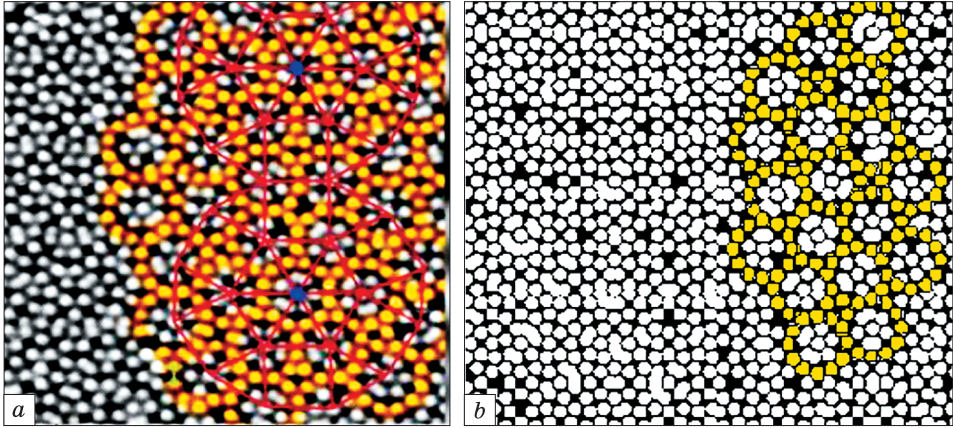


Fig. 19. Comparison of atomic structure of BaTiO₃ thin layer on platinum substrate (a) [53] and fragment of group D_5 (b) (algorithm (61))

here, $a_{4D} = 2/(\sqrt{3}a_{4D}^*)$ is a lattice parameter. Denoting the interplanar distance corresponding the basis vector of reciprocal lattice as d_q and considering that $a_{4D}^*/\sqrt{2} = 1/d_q$, we obtain the equation for the parameter of four-dimensional lattice and quasi-parameter a of four-dimensional quasi-lattice:

$$a_{4D} = d_q \sqrt{2/3}, \quad a = a_{4D}/\sqrt{2} = d_q/\sqrt{3}. \quad (58)$$

Then, to calculate the interplanar distances, we can use expression

$$d_{(N^*, M^*)} = a\sqrt{3}/\sqrt{N^* + M^*\sqrt{3}}. \quad (59)$$

If there were detected reflexes corresponding to basis vectors, which are closely located to primary electron beam, then, equation remains similar to Eq. (59):

$$d_{(N_{ch}, M_{ch})} = a_{ch}\sqrt{3}/\sqrt{N_{ch} + M_{ch}\sqrt{3}}, \quad (60)$$

where $a_{ch} = a\sqrt{7 + 4\sqrt{3}} = a t_1$.

From the physical point of view, (N^*, M^*) indices are more correct, since they relate to the fundamental vectors of the reciprocal quasi-crystal lattice. However, indices (N_{ch}, M_{ch}) are more convenient, because, if we know only one index from this pair, we can easily determine the second index and estimate the intensity of the corresponding reflections (see Eq. (56)).

Thus, the dodecagonal system ‘falls out’ of the general relation $|Q^\perp|^2 \propto (Nk - M)$; this is observed for other existing types of quasi-crystals. However, it is still possible to indexing diffraction reflections us-

ing integers. At the same time, taking into account the periodicity of dodecagonal quasi-crystals along the 12th-order symmetry axis, all diffraction peaks on the powder diffraction patterns can be indexed with three indices, as for the octagonal and decagonal quasi-crystals.

Except the analysis of the diffraction pattern from quasi-crystalline materials, the description and classification of quasi-crystalline structure is a complicated problem. We proposed above the method for description of the variety of octagonal quasi-lattices. Such description is possible because we can change the coefficients of vectors in initial algorithm (42). For example, a change of even one coefficient changes the quasi-lattice without affecting its symmetry. For instance, the image of the atomic structure of a thin BaTiO₃ layer on a platinum substrate was obtained in Ref. [53]. We obtained almost the same geometry of the arrangement of sites (Fig. 19) using the following algorithm:

$$\begin{aligned} D_2 &= D_1 + \{2t^{-1}\mathbf{q}_i\}D_1, & D_3 &= D_2 + \{2\mathbf{q}_i\}D_2, \\ D_4 &= D_3 + \{t\mathbf{q}_i\}D_3, & D_5 &= D_4 + \{2t\mathbf{q}_i\}D_4. \end{aligned} \quad (61)$$

Taking into account earlier proposed denotation of quasi-crystalline structures classes, the structure illustrated in Fig. 18 can be denoted as $D(2/t, 2, t, 2t)$.

5. Conclusions

The method of modelling the quasi-periodic structures, which act as a geometric interpretation of Fibonacci-type sequences, is proposed.

The correspondence between projection method for periodic lattices and the method of recurrent multiplication of basis sites' group is obtained.

The possibility of using only three indices (*NML*) for describing diffraction patterns for quasi-crystals with 10th-order, 8th-order, and 12th-order symmetry axis is proved.

Using constructed algorithm for quasi-crystalline structures, we can directly obtain information about the intensity of diffraction reflexes.

Described method of modelling is simpler as compared with projection method. It enables to operate the coordinates of two-dimensional space unlike to coordinates with dimensionality, greater than three.

REFERENCES

1. J.W. Cahn, D. Shechtman, and D. Gratias, *J. Mater. Res.*, **1**, No. 1: 30 (1986).
<https://doi.org/10.1557/JMR.1986.0013>
2. A. Katz and M. Duneau, *Scr. Metall.*, **20**, No. 9: 1211 (1986).
[https://doi.org/10.1016/0036-9748\(86\)90033-5](https://doi.org/10.1016/0036-9748(86)90033-5)
3. D. Levine and P.J. Steinhardt, *Phys. Rev. B*, **34**, No. 2: 596 (1986).
<https://doi.org/10.1103/PhysRevB.34.596>

4. S. Ebalard and F. Spaepen, *J. Mater. Res.*, **4**, No. 1: 39 (1989).
<https://doi.org/10.1557/JMR.1989.0039>
5. J. Socolar, *Phys. Rev. B*, **39**, No. 15: 10519 (1989).
<https://doi.org/10.1103/PhysRevB.39.10519>
6. W. Bogdanowicz, *Cryst. Res. Technol.*, **38**, Nos. 3–5: 307 (2003).
<https://doi.org/10.1002/crat.200310036>
7. W. Bogdanowicz, *Cryst. Res. Technol.*, **40**, Nos. 4–5: 488 (2005).
<https://doi.org/10.1002/crat.200410372>
8. D.A. Shulyatev, *Crystallogr. Rep.*, **52**, No. 6: 938 (2007).
<https://doi.org/10.1134/S106377450706003X>
9. W. Steurer, T. Haibach, and B. Zhang, *Acta Cryst. B*, **49**: 661 (1993).
<https://doi.org/10.1107/S0108767393001758>
10. A. Yamamoto and K. N. Ishihara, *Acta Cryst. A*, **44**: 707 (1988).
<https://doi.org/10.1107/S0108767388002958>
11. P. Schall, M. Feuerbacher, and K. Urban, *Phys. Rev. B*, **69**, No. 13: 134105 (2004).
<https://doi.org/10.1103/PhysRevB.69.134105>
12. Y. Yan, R. Wang, J. Gui, and M. Dai, *Acta Cryst.*, **49**: 435 (1993).
<https://doi.org/10.1107/S0108768192010127>
13. X.B. Liu, G. C. Yang, J.F. Fan, and G.S. Song, *J. Mater. Sci. Lett.*, **22**, No. 2: 103 (2003).
<https://doi.org/10.1023/A:1021850417176>
14. X.B. Liu, *J. Mater. Sci.*, **38**, No. 5: 885 (2003).
<https://doi.org/10.1023/A:1022300503414>
15. G. Rosas, C. Angeles-Chavez, and R. Perez, *J. New Mater. Electrochem. Syst.*, **8**: 149 (2005).
16. M. Boström and S. Hovmöller, *Solid State Chem.*, **153**, No. 2: 398 (2000).
<https://doi.org/10.1006/jssc.2000.8790>
17. Z.M. Mo and K.H. Kuo, *Mater. Sci. Eng.*, **294–296**: 242 (2000).
[https://doi.org/10.1016/S0921-5093\(00\)01333-2](https://doi.org/10.1016/S0921-5093(00)01333-2)
18. Y. Vekilov and M. Chernikov, *Phys.-Usp.*, **53**: 537 (2010).
<https://doi.org/10.3367/UFNr.0180.201006a.0561>
19. J.S. Wu and K.H. Kuo, *Metall. Mater. Trans. A*, **28**, No. 3: 729 (1997).
<https://doi.org/10.1007/s11661-997-0059-9>
20. V. Elser, *Phys. Rev. B*, **32**, No. 8: 4892 (1985).
<https://doi.org/10.1103/PhysRevB.32.4892>
21. V.V. Girzhon, V.M. Kovalyova, O.V. Smolyakov, and M.I. Zacharenko, *J. Non-Cryst. Solids*, **358**: 137 (2012).
<https://doi.org/10.1016/j.jnoncrsol.2011.09.017>
22. V.V. Girzhon, O.V. Smolyakov, and I.V. Gayvoronsky, *Sposib Modelyuvannya Struktury Dodekagonalnykh Kvazykrystaliv*: Patent No. 80699 MPK G09B 23/26 G09B 23/06 (Patent na korysnu model No. 11) (2012) (in Ukrainian).
23. V.V. Girzhon, O.V. Smolyakov, and M.I. Zakharenko, *ZhETF*, **5**, No. 11: 973 (2014).
<https://doi.org/10.7868/S0044451014110091>
24. O.V. Smolyakov and V.V. Girzhon, *ZhETF*, **3**, No. 9: 521 (2017).
<https://doi.org/10.7868/S0044451017090097>
25. V.V. Girzhon, O.V. Smolyakov, and I.V. Gayvoronsky, *Visnyk Lvivskogo Universytetu. Seriya Fizychna*, **54**: 13 (2017).
26. S. Ritsch, *Philos. Mag. Lett.*, **74**, No. 2: 99 (1996).
<https://doi.org/10.1080/095008396180452>
27. S.A. Ranganathan, E.A. Lord, N.K. Mukhopadhyay, and A. Singh, *Acta Cryst. A*, **63**, No. 1: 1 (2007).
<https://doi.org/10.1107/S0108767306041298>

28. J. Dubois, *Useful Quasicrystals* (Singapore–London: World Scientific: 2005).
29. M.A. Bicknell, *The Fibonacci Quart*, **13**, No. 4: 345 (1975).
30. S. Burkov, *Phys. Rev. B*, **47**: 12325 (1993).
<https://doi.org/10.1103/PhysRevB.47.12325>
31. W. Steurer and S. Deloudi *Crystallography of Quasicrystals: Concepts, Methods and Structures* (London–New York: Springer: 2009).
32. R. Amman, B. Grünbaum, and G. Shephard, *Discrete & Computational Geometry*, **8**, No. 1: 1 (1992).
33. F.P.N. Beenker, *Algebraic Theory of Non-Periodic Tilings of the Plane by Two Simple Building Blocks: a Square and a Rhombus* (Eindhoven: Eindhoven University of Technology: 1982).
34. C. Janot, *Quasicrystals* (Oxford: Oxford Clarendon Press: 1994).
35. Y. Roichman and D. Grier, *Holographic Assembly of Quasicrystalline Photonic Heterostructures* (New York: Department of Physics and Center for Soft Matter Research: 2005).
36. W. Steurer and S. Deloudi, *Crystallography of Quasicrystals: Concepts, Methods and Structures* (London–New York: Springer: 2009).
37. D. Levine, P. Steinhardt, *Phys. Rev. Lett.*, **53**: 2477 (1984).
<https://doi.org/10.1103/PhysRevLett.53.2477>
38. K. Kuo, *J. Non-Cryst. Solids*, **117–118**: 756 (1990).
[https://doi.org/10.1016/0022-3093\(90\)90639-4](https://doi.org/10.1016/0022-3093(90)90639-4)
39. H. Chen, D.X. Li, and K.H. Kuo, *Phys. Rev. Lett.*, **60**, No. 16: 1645 (1988).
<https://doi.org/10.1103/PhysRevLett.60.1645>
40. T. Ishimasa, H.-U. Nissen, and Y. Fukano, *Phys. Rev. Lett.*, **55**, No. 5: 511 (1985).
<https://doi.org/10.1103/PhysRevLett.55.511>
41. K. Yoshida, T. Yamada, and Y. Taniguchi, *Acta Cryst. B*, **45**: 40 (1989).
<https://doi.org/10.1107/S0108768188011024>
42. M. Uchida and S. Horiuchi, *J. Appl. Cryst.*, **31**: 634 (1998).
<https://doi.org/10.1107/S0021889898003008>
43. H. Iga, M. Mihalkovic, and T. Ishimasa, *Philos. Mag.*, **91**, Nos. 19–21: 2624 (2011).
<https://doi.org/10.1080/14786435.2010.508448>
44. X. Zeng, G. Ungar, Y. Liu, V. Percec, A.E. Dulcey, and J.K. Hobbs, *Nature*, **428**: 157 (2004).
<https://doi.org/10.1038/nature02368>
45. S. Fischer, A. Exner, K. Zielske, J. Perlich, S. Deloudi, W. Steurer, P. Lindner, and S. Förster, *Proc. Natl. Acad. Sci. U.S.A.*, **108**, No. 5: 1810 (2011).
<https://doi.org/10.1073/pnas.1008695108>
46. K. Hayashida, T. Dotera, and A. Takano, *Phys. Rev. Lett.*, **98**, No. 19: 195502-1 (2007).
<https://doi.org/10.1103/PhysRevLett.98.195502>
47. A.E. Madison, *Struct. Chem.*, **26**, No. 4: 923 (2015).
<https://doi.org/10.1007/s11224-014-0559-3>
48. S. Iwami and T. Ishimasa, *Philos. Mag. Lett.*, **95**, No. 4: 229 (2015).
<https://doi.org/10.1080/09500839.2015.1038332>
49. M. Conrad, F. Krumeich, and B. Harbrecht, *Angew. Chem. Int. Ed.*, **37**, No. 10: 1383 (1998).
[https://doi.org/10.1002/\(SICI\)1521-3773\(19980605\)37:10<1383::AID-ANIE1383>3.0.CO;2-R](https://doi.org/10.1002/(SICI)1521-3773(19980605)37:10<1383::AID-ANIE1383>3.0.CO;2-R)
50. B. Souvignier, *Acta Cryst. A*, **59**: 210 (2003).
<https://doi.org/10.1107/s0108767303004161>
51. P.A. Bancel, *Phys. Rev. Lett.*, **54**, No. 22: 2422 (1985).
<https://doi.org/10.1103/PhysRevLett.54.2422>

52. F. Gähler, *Quasicrystalline Materials. Proc. I.L.L. / Codest Workshop, Grenoble, 21–25 March 1988* (Singapore: World Scientific: 1988), p. 272.
53. S. Förster, K. Meinel, R. Hammer, M. Trautmann, and W. Widdra, *Nature*, **502**: 215 (2013).
<https://doi.org/10.1038/nature12514>

Received June 14, 2019;
in final version, October 10, 2019

В.В. Гіржон, О.В. Смоляков

Запорізький національний університет,
вул. Жуковського, 66, 69600 Запоріжжя, Україна

МОДЕЛЮВАННЯ ҐРАТНИЦЬ ДВОВИМІРНИХ КВАЗИКРИСТАЛІВ

Запропоновано спосіб моделювання квазіперіодичних структур, в основі якого лежить алгоритм, що є геометричною інтерпретацією числових послідовностей типу послідовності Фібоначчі. Моделювання полягає у рекурентному розмноженні базисних груп вузлів, які мають ротаційну симетрію 10, 8 або 12-го порядку. Перевагою запропонованого способу є можливість оперувати координатами лише двовимірного простору, а не гіпотетичних просторів із вимірністю, вищою за три. Показано відповідність між методом проєціювання періодичних ґратниць і методом рекурентного розмноження груп базисних вузлів. Встановлено, що шестивимірну обернену ґратницю для декагонального квазикристалу можна одержати з ортогональної шестивимірної ґратниці для ікосаедричного квазикристалу за допомогою зміни масштабу вздовж одного з базисних векторів і заборони на проєціювання вузлів, для яких сума п'ятьох індексів (відповідних іншим базисним векторам) не дорівнює нулю. Показано достатність використання лише трьох індексів для опису дифрактограм від квазикристалів з осями симетрії 10, 8 та 12-го порядків. Оригінальний алгоритм уможливорює безпосереднє одержання інформації про інтенсивність дифракційних рефлексів за кількістю самонакладань вузлів у процесі побудови обернених ґратниць квазикристалів.

Ключові слова: квазіперіодичні структури, послідовність Фібоначчі, метод проєціювання, базисні вектори, ротаційна симетрія, обернена ґратниця.

В.В. Гиржон, А.В. Смоляков

Запорожский национальный университет,
ул. Жуковского, 66, 69600 Запорожье, Украина

МОДЕЛИРОВАНИЕ РЕШЁТОК ДВУМЕРНЫХ КВАЗИКРИСТАЛЛОВ

Предложен способ моделирования квазипериодических структур, в основе которого лежит алгоритм, являющийся геометрической интерпретацией числовых последовательностей типа последовательности Фибоначчи. Моделирование заключается в рекуррентном размножении базисных групп узлов, имеющих ротационную симметрию 10, 8 или 12-го порядка. Преимуществом предлагаемого способа является возможность оперировать координатами только двумерного пространства, а не гипотетических пространств с размерностью, большей трёх. Показано соответствие между методом проецирования периодических решёток и методом рекуррентного размножения групп базисных узлов. Установлено, что шестимерную обратную решётку для декагональных квазикристаллов можно

получить из ортогональной шестимерной решётки для икосаэдрических квазикристаллов с помощью изменения масштаба вдоль одного из базисных векторов и запрета на проецирование узлов, для которых сумма пяти индексов (соответствующих другим базисным векторам) не равна нулю. Показана достаточность использования только трёх индексов для описания дифрактограмм от квазикристаллов с осями симметрии 10, 8 и 12-го порядков. Оригинальный алгоритм даёт возможность непосредственного получения информации об интенсивности дифракционных рефлексов по количеству самоналожений узлов в процессе построения обратных решёток квазикристаллов.

Ключевые слова: квазипериодические структуры, последовательность Фибоначчи, метод проецирования, базисные векторы, ротационная симметрия, обратная решётка.